P9.10 OPERATIONAL APPLICATION OF 0-3 KM BULK SHEAR VECTORS IN ASSESSING QLCS MESOVORTEX AND TORNADO POTENTIAL

Jason S. Schaumann*
NOAA/National Weather Service, Springfield, MO

Ron W. Przybylinski
NOAA/National Weather Service, St. Charles, MO

1. INTRODUCTION

Quasi-linear Convective Systems (QLCSs) have presented a challenge to critical weather operations in all sectors of meteorology for decades. The propensity for these systems to produce swaths of wind damage has been a heavily researched topic stemming as far back as the 1950s. Fujita (1978) documented the structure and time evolution of radar signatures he coined as a "bow echo". Rapidly propagating severe bow echoes have also been shown to result in significant property damage and loss of life (e.g., Fujita and Wakimoto 1981; Johns and Hirt 1987; Przybylinski 1995, hereafter P95). Fujita first hypothesized that the descending nature of the rear-inflow jet (RIJ) near the apex of a developing bow was a primary cause for swaths of wind damage. Early and recent radar and observational studies, as well as numerical simulations (e.g., Forbes and Wakimoto 1983; Schmidt and Cotton 1989; Houze et al. 1989; Burgess and Smull 1990; Jorgensen and Smull 1993; P95; Funk et al. 1999, hereafter F99; Atkins et al. 2004, hereafter A04) have confirmed that these larger swaths of wind damage can be traced back to bow echoes associated with a descending mesoscale RIJ. Radar characteristics associated with the early stages of bow segments include the expanding rear inflow notch (RIN) along the trailing flank of the system, strong low-level reflectivity gradients along the leading edge, and the mid-altitude radial convergence (MARC) signature (Przybylinski et al. 1995; Schmocker et al. 1996). These signatures are precursors to swaths of damaging winds and the descent of a RIJ. These precursors have allowed warning meteorologists to provide increased lead time and accuracy in the issuance of Severe Thunderstorm Warnings.

Recent studies have shown that mesovortices can also produce localized swaths of (E)F-0 to (E)F-1 wind damage (e.g., Atkins et al. 2005, hereafter A05; Wakimoto et al. 2006b; Wheatly et al. 2006). They are also responsible for the production of tornadoes (e.g., P95; F99; Przybylinski et al. 2000; A04; A05). While the majority of tornadoes tend to be classified in the (E)F-0 to (E)F-1 category, damage assessments have revealed damage intensity as high as the (E)F-3 and (E)F-4 range (Trapp et al. 2005). Trapp et al. (1999) also showed that tornadogenesis emanating from mesovortices often occurs much quicker than those from supercells, with a mean lead time of approximately five minutes. While an overwhelming amount of research has been conducted on the topic of environments and physical processes which lead to supercell tornadogenesis (e.g., Burgess 1974; Rasmussen 2003, hereafter R03; Thompson et al. 2003; Markowski et al. 2008), research on environmental settings for QLCS tornadoes has been limited to mainly case studies (e.g., Przybylinski et al. 1996; A04; A05).

We have examined radar and environmental data for several progressive mesoscale convective system (MCS) cases dating back to 2004 from the eastern High Plains through the Atlantic coast from both the cold (October to March) and warm (April to September) seasons. Three environmental parameters were investigated including 0-3 km bulk shear, most unstable CAPE, and 0-3 km theta-e differential. Examination of these cases has revealed *three co-existing ingredients* which support an increased likelihood for QLCS mesovortex genesis and strong intensification, both from an environmental and radar characteristic standpoint:

1) A portion of a QLCS in which the system cold pool and ambient low-level shear are nearly balanced or slightly shear dominant.
2) Where 0-3 km line-normal bulk shear magnitudes are equal to or greater than 15 m s^{-1} (30 knots).
3) Where a RIJ or enhanced outflow causes a surge or bow in the line.

The first section of this paper will primarily focus on the selection, role, and application of 0-3 km bulk shear vectors given their relationship to the first two ingredients listed above. The second portion of the paper will apply the 0-3 km shear vector methodology to three case studies, with examples of line surges and bows (the third ingredient) also presented. The first case occurred during the overnight hours of 26-27 June 2011 and produced significant wind damage from southern Iowa through northeastern and parts of east-central Missouri and into west-central Illinois. Multiple weak tornadoes occurred over parts of northeastern Missouri with this case. The second case occurred during the late evening and early overnight hours of 18-19 June 2011. A small forward propagating bow echo moved eastward and spawned three weak tornadoes on the

* *Corresponding Author's Address:* Jason Schaumann, NOAA/National Weather Service, Springfield, MO.
E-mail: Jason.Schaumann@noaa.gov

north side of the bow 15 miles northwest of Springfield, Missouri and a stronger tornado approximately 30 miles south-southeast of Rolla, Missouri over southern Crawford County. The third case is the 19 July 2006 derecho in which numerous swaths of damaging downburst and microburst winds occurred from southeastern Minnesota through central Illinois, then south-southwest through the St. Louis metropolitan area, and finally into south-central Missouri and north-central Arkansas. Surface wind gusts were as high as 30 to 35 m s^{-1} with this event.

2. BACKGROUND AND APPLICATION

a. Mesovortex Genesis

The development of mesovortices has been simulated numerically (e.g., Trapp and Weisman 2003, hereafter TWII03; Atkins and St. Laurent 2009b, hereafter ALII09), although the exact genesis mechanisms for these features remains a topic of debate. One commonality in these numerical simulations linked the genesis of mesovortices to the tilting and stretching of horizontal vorticity in the vicinity of the updraft/downdraft convergence zone (UDCZ). Rotunno et al. (1988, hereafter RKW88) showed that low-level shear balanced with horizontal vorticity generated by the system cold pool produced deep, upright updrafts. The presence of deep and upright updrafts along the UDCZ acts to maximize vortex stretching potential (ALII09) (Figure 1). One unexplored environmental parameter for QLCS mesovortex genesis is the potential contribution to parcel buoyancy and upward acceleration from thermodynamic instability in the low-levels. The utility of 0-3 km CAPE has been explored (e.g., R03; Davies 2006a) in assessing the likelihood of supercell tornadogenesis. Future exploration in the area of low-level CAPE in QLCS tornadogenesis is encouraged.

ALII09 depicted that the buoyancy gradient across a gust front produces horizontal vorticity which is subsequently tilted and stretched by the updraft. Convective-scale downdrafts tend to produce localized surges or bulges within the early stages of a QLCS. In contrast, a RIJ typically results in a larger bow echo signature during the mature stage of a MCS. Localized surges may also occur within a larger bow echo due to contributions from a descending RIJ and convective downdrafts. Our observations and numerical simulations have shown that *stronger mesovortices tend to occur along or just behind the gust front within the theta-e gradient region and in the presence of a line surge or bow echo*.

Simulations conducted by Weisman and Trapp (2003, hereafter WTI03) revealed that significant, low-level cyclonic vortices were produced within QLCSs when unidirectional shear magnitudes equaled or exceeded 20 ms^{-1} over the lowest 2.5 and 5 km AGL layers. These vortices tended to be long-lived, stronger, and deeper. Other simulations completed by Atkins and St. Laurent (2009a) used varying amounts of shear within the 0-2.5 and 0-5.0 km layers and showed that weaker, short-lived, and shallow mesovorticies formed with shear values of less than 15 m s^{-1}.

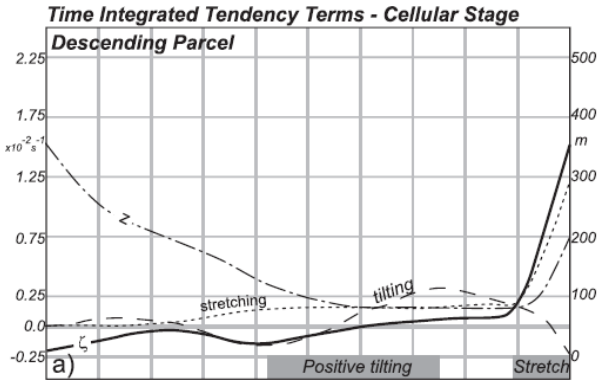

FIG. 1. From ALII09. Time series of integrated vertical vorticity tendency term (s^{-1}) for a parcel which populates a mesovortex. Vertical vorticity (ζ) increases rapidly as stretching occurs in the updraft.

b. Shear/Cold Pool Balance

In the absence of low-level wind shear, a convective cold pool will theoretically spread out equally in all directions due to horizontal pressure gradients. Additionally, the cold pool will tend to spread faster near the surface. The advancement of a cold pool creates a rotor of horizontal vorticity in the lower atmosphere (Figure 2). The depth of this horizontal rotor is highly dependent on the depth of the cold pool. Bryan et al. (2005, hereafter B05) used soundings taken within cold pools to show that depths greater than 3 km may be common. Given that real-time measurements of cold pool depth are typically not available, an approximation is often necessary. Our research has found that 3 km serves as a good approximation of cold pool depth along the advancing edge. Cold pool depth would tend to increase farther back into the cold pool (Figure 2) and may be more consistent with the findings of Bryan et al.

While the orientation of the horizontal vorticity rotors can be inferred in a physical sense, one must also account for the strength of the cold pool to determine the amount of horizontal vorticity present. RKW88 showed that cold pool strength dictates the propagation speed of the cold pool. We will present a quantitative and qualitative way to determine cold pool strength later in this document.

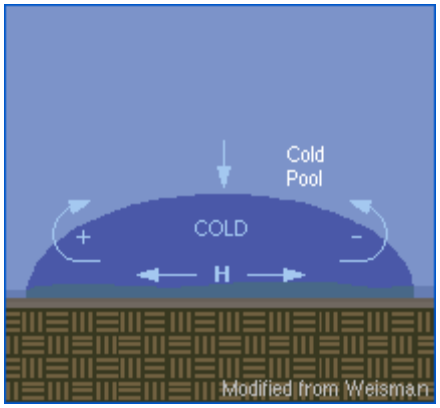

FIG. 2. Two dimensional schematic of an expanding cold pool. Horizontal vorticity rotors are depicted on either side of the cold pool. Graphic courtesy of COMET.

In similar fashion, the presence of low-level ambient shear also results in horizontal vorticity. Given a unidirectional wind profile, increasing winds speeds with height will result in a horizontal vorticity rotor orientated perpendicular to the wind direction (Figure 3). For westerly winds which increase with height, the resulting horizontal vorticity vector would be pointed to the north.

The orientation and strength of both cold pool and low-level shear induced horizontal vorticity then becomes critical in determining shear and cold pool balance. The ability of a MCS to generate new updrafts is maximized when the horizontal vorticity from both the cold pool and low-level shear are of equal magnitude and where the edges of both "converging" horizontal rotors are rotating in an upwards fashion (Figure 4). The convergence of these horizontal rotors is also commonly referred to as the UDCZ. In Figure 4, the net upward motion along the UDCZ would be greatly increased due to upward contributions from both rotors. This interaction is commonly referred to as constructive interference.

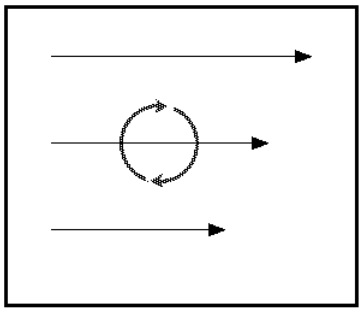

FIG. 3. Two-dimensional depiction of horizontal shear vorticity. Graphic courtesy of Doswell (2000).

Using the orientation of horizontal vorticity induced by both the system cold pool and low-level environmental shear, RKW88 classified three different shear and cold pool balance regimes. One regime depicts a system cold pool that overpowers ambient low-level shear (herein referred to as a "cold pool dominant" regime). A second regime presented shows the system cold pool in balance with ambient low-level shear (herein referred to as a "balanced" regime). The final regime depicts ambient low-level shear overpowering the system cold pool (herein referred to as a "shear dominant" regime) (Figure 5).

As can be seen in Figure 5, a much deeper and upright updraft is present in a balanced regime. Our observations along with numerical simulations have shown that *a balanced or slightly shear dominant regime results in increased mesovortex development and maximizes tilting and stretching of vorticity near the UDCZ*. The probability of new updraft development along an advancing cold pool is also maximized in a balanced regime given a greater likelihood of parcels overcoming the level of free convection (LFC). Near-surface parcels may still ascend and overcome the LFC in either a cold pool dominant or shear dominant regime given a weak capping inversion or low LFC.

Throughout our research, we have noted numerous instances where multiple regimes were present within the same QLCS. In rare instances such as the 8 May 2009 super-derecho (Figure 6), all three regimes were observed simultaneously. Additionally, these regimes tend to change throughout the maturation process of a QLCS. Thus, it is critical for radar operators to continually assess the state of shear/cold pool balance throughout all sections of an ongoing QLCS.

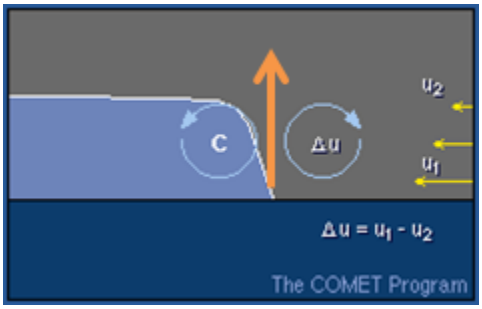

FIG 4. Interaction of cold pool and low-level shear rotors resulting in constructive inteference. Graphic courtesy of COMET.

c. Application

While radar imagery and surface observations provide potential clues to the state of shear/cold pool balance contained within a QLCS, we introduce additional methods to determine the balance in a near real-time sense. The first method attempts to quantify the strengths of the system cold pool and ambient low-level shear. These two quantities are then compared to determine regime type. A second method compares radar imagery and 0-3 km bulk shear vectors to the

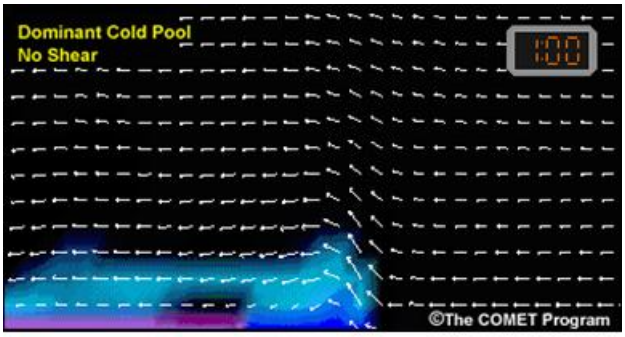

Updrafts in a cold pool dominant regime tend to be weaker and rearward leaning. The horizontal vorticity rotor generated by the system cold pool tends to pull parcels ahead of the advancing gust front up and over the cold pool.

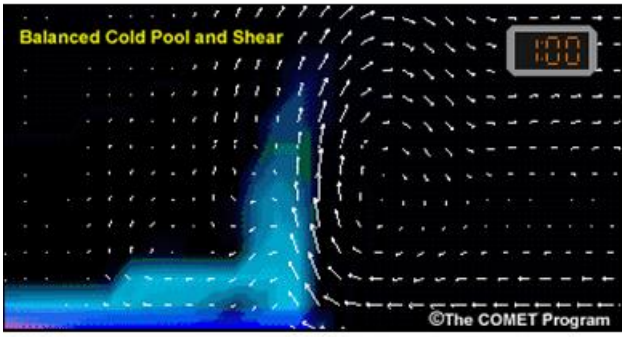

Updrafts in a balanced regime tend to be vertically deep and upright. The constructive interference between the system cold pool and low-level shear is maximized.

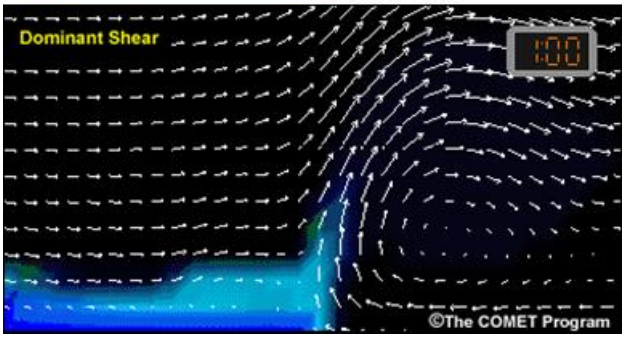

Updrafts in a shear dominant regime tend to be weaker and slightly forward leaning. The horizontal vorticity rotor generated by ambient low-level shear tends to pull parcels from the leading edge of the cold pool downshear.

FIG. 5. Three distinct shear/cold pool regimes depicted by Weisman and Przybylinski (1999) through COMET. White arrows represent two-dimensional motions of air parcels. Blue shading represents the system cold pool.

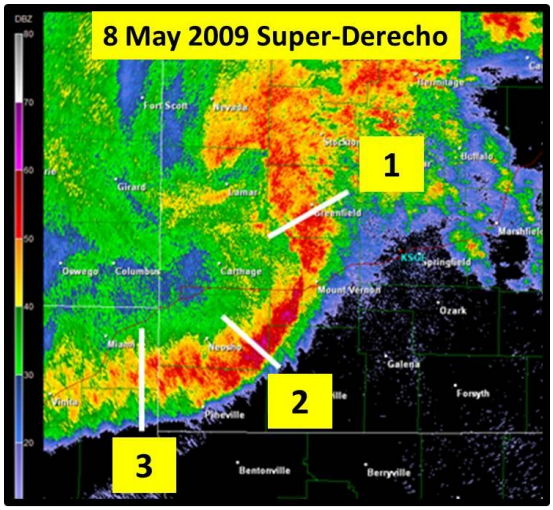

FIG. 6a. Legend depicting cross-section segments for the 8 May 2009 super-derecho. Radar image created with Gibson Ridge Level 2 software.

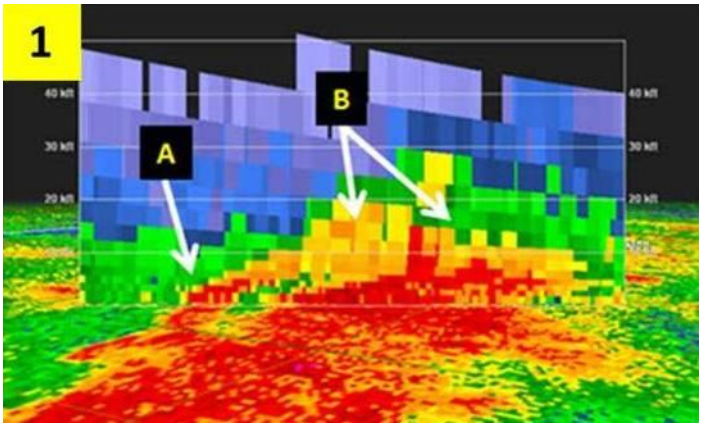

Segment 1 reflectvity cross-section. The orientation of the cross-section is from the rear to the front of the convective line. This portion of the line is **shear dominant** featuring little vertical growth to updrafts and both trailing and leading stratiform preciptation. Arrow "A" points to a thin and forward leaning updraft along the UDCZ. The arrows in "B" point to intense leading stratiform precipitation.

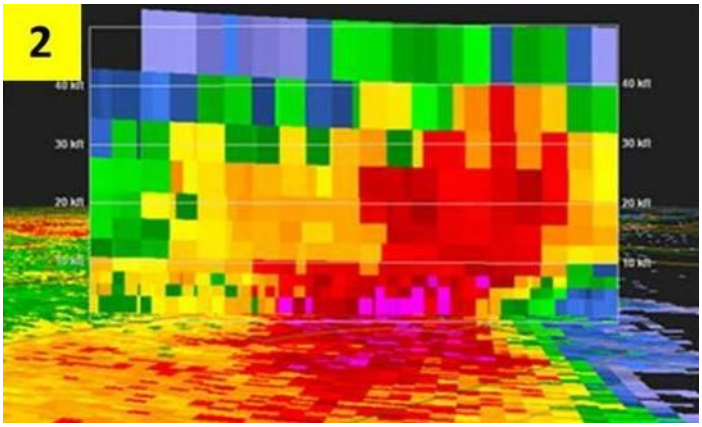

Segment 2 reflectvity cross-section. The orientation of the cross-section is from the rear to the front of the convective line. This portion of the line is nearly **balanced** featuring intense and upright updrafts up to 40 kft AGL, along with a strong reflectivity gradient at the leading edge. This segment also features trailing stratiform precipitation.

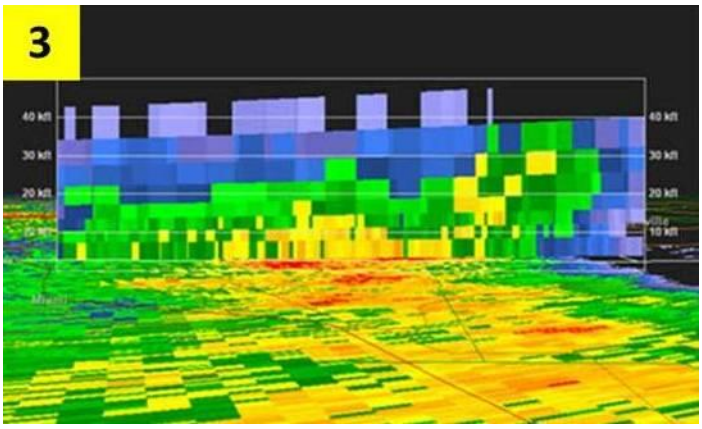

Segment 3 reflectvity cross-section. The orientation of the cross-section is from the rear to the front of the convective line. This portion of the line is **cold pool dominant** featuring little vertical growth to updrafts and trailing stratiform preciptation. Also notice on the plan view image the weak returns (near #3 segment label) ahead of the line, likely indicating a gust front outrunning the main convection.

FIG. 6b. Reflectivity cross-sections depicting 3 distinct shear/cold pool balance regimes which were simultaneously present during the 8 May 2009 super-derecho. Radar images created with Gibson Ridge Level 2 software.

three shear/cold pool balance conceptual models presented by RKW88.

The magnitude and orientation of low-level horizontal vorticity can be quantified by calculating the amount of shear present. Since wind profiles are often not unidirectional, bulk shear vectors best represent orientation and strength of horizontal vorticity in the ambient atmosphere. As a proxy, the low-level bulk shear layer selected should approximately match the depth of the advancing edge of a system cold pool. As we stated earlier in this paper, we have found that the 0-3 km layer serves as a good approximation.

One important finding of our research has been the utility of the line-normal component of 0-3 km bulk shear vectors. Cohen et al. (2007) tested the system-normal component of various layers of bulk shear to classify the strength of past MCSs. Communication with the authors of this paper indicate that they used a mean orientation of the system to calculate these quantities. We have taken this approach a step further and compared 0-3 km bulk shear vectors to the orientation of all convective segments contained within QLCSs. More specifically, we have compared the orientation and magnitude of these vectors to the UDCZ throughout the entire expanse of each QLCS. Given that individual segments within a QLCS often exhibit differing orientations and forward speeds, we feel that this method results in a better representation of the low-level horizontal vorticity available to interact with individual line segment cold pools contained within the parent QLCS.

The calculation for 0-3 km line-normal bulk shear (**Δu**) is rather straight forward,

$$\Delta u = \sin(\theta)m, \quad (1)$$

where **θ** is the angle between the convective line and 0-3 km bulk shear vector, and **m** is the magnitude of the 0-3 km bulk shear vector.

When calculating line-normal magnitudes, one must ensure that the vectors are representative of the ambient atmosphere ahead of the convective line. Model output will likely be unrepresentative if the convective scheme is generating precipitation. Radar operators should look downstream of the model generated precipitation to gauge the orientation and magnitude of true ambient vectors. In real-time operations, the use of downstream RAOBs, velocity azimuth display (VAD) wind profiles, and vertical wind profilers may be beneficial.

While the computation of ambient low-level shear is rather simple given that bulk shear vectors are readily plotted or available, the calculation of cold pool strength is not nearly as straight forward. RKW88 showed that the strength of the cold pool circulation can be approximated using the speed of the cold pool propagation. The strength of the advancing cold pool (**c**) can be calculated using pressure rises as the cold pool passes over a given location using the equation

$$c \approx \left(2\frac{\Delta p}{\bar{\rho}}\right)^{1/2}, \quad (2)$$

where **Δp** is the cold pool pressure rise (kg/ms^2 or mb × 10^{-2}), and $\bar{\rho}$ is the density of a standard atmosphere (1kg/m^3). Using Equation 2, one can then approximate the cold pool strength for various pressure rises.

There are several potential drawbacks to using this method from both a meteorological and observational standpoint: 1) this method does not allow contributions to the pressure at the surface due to pressure perturbations above the cold pool and 2) the current density of the surface observation network is often not sufficient to capture the true magnitude of cold pool pressure rises. The Wichita and Springfield Weather Forecast Offices (WFOs) have used a modified version of this equation to approximate cold pool strength. Similar to findings in B05, reducing the cold pool strength calculated in Equation 2 by 50% appears more representative of system cold pool behavior (See Table 1).

MSLP Pressure Change (mb)	Cold Pool Strength (m s^{-1})
1	7
2	10
3	13
4	14
5	16
6	18
7	19
8	21
9	22
10	23

TABLE 1. Calculated theoretical cold pool shear strengths using equation (2). Table is courtesy of Ken Cook (Science and Operations Officer at the NWS Forecast Office in Wichita, KS).

When determining a cold pool pressure rise, the pressure minimum downshear of the gust front is subtracted from the maximum pressure rise as the cold pool settles over an observation site. Several observation sites should be examined to determine the maximum cold pool pressure rise. This method of cold pool calculation should be utilized in the absence of any significant low-level forcing, since isallobaric tendencies in forcing situations tend to be heavily modulated by synoptic-scale mechanisms. Additionally, the forcing mechanism itself often replaces the thermodynamically driven cold pool due to convergence along the forcing feature.

The cold pool strength term derived from Table 1 can then be compared to the line-normal magnitude of 0-3 km bulk shear. Values of near equal magnitude would constitute a line segment in a near balanced

state. Greater(lesser) magnitudes of cold pool strength indicate a cold pool dominant(shear dominant) line segment.

While 0-3 km bulk shear vectors are an important tool in assessing the state of shear and cold pool balance, we have also found that increasing bulk shear magnitudes over this layer leads to greater mesovortex potential. Our observations indicate that *line-normal magnitudes equal to or greater than 15 m s^{-1} correlate to an increasing likelihood for mesovortex genesis and tornadoes*. Past observational research (e.g., F99; DeWald and Funk 2000) also identified increased mesovortex genesis and tornado production when low-level shear values were equal to or greater than 15 m s^{-1}.

While the physical significance of the 15 m s^{-1} 0-3 km bulk shear threshold is not clear, perhaps one explanation may be the relationship of shear and cold pool balance. Engerer et al. (2008, hereafter E08) used the Oklahoma Mesonet network to sample cold pool pressure rises from 39 MCSs. They found that the mean cold pool pressure rise during MCS initiation was 4 mb, while the mean pressure rise during the mature phase of MCSs was 4.5 mb (Figure 7). Comparing these values to Table 1, theoretical shear values needed to "balance" this cold pool strength would be around 14-16 m s^{-1}. Thus, it is possible that 0-3 km bulk shear values around 15 m s^{-1} represent the low-level ambient shear needed to balance a typical cold pool. Using the mean cold pool pressure rises from E08 during the development to mature stages of a MCS, 0-3 km bulk shear values of less than 15 m s^{-1} would often support a cold pool dominant MCS with a correspondingly lower potential for mesovortex development. Further research is planned on assessing the statistical significance of the 15 m s^{-1} 0-3 km bulk shear threshold.

Given the drawbacks outlined earlier in quantifying the true strength of a system cold pool in a real-time sense, we have found much greater success using 0-3 km bulk shear vector plots in conjunction with radar imagery. Comparison of the low-level UDCZ depicted on a 0.5° storm relative motion (SRM) product to 0.5° reflectivity (Z) can readily highlight differing shear and cold pool balance regimes (Figure 8). Radar cross sections, all-tilts displays, and other radar products can also be valuable tools for depicting shear and cold pool balance.

<u>Indicators of a cold pool dominant line segment</u>

1) UDCZ or gust front is outrunning the main convection.
2) Radar cross-section or all-tilts displays indicate updrafts are leaning rearward with less vertical development.
3) Trailing stratiform precipitation.

<u>Indicators of a balanced line segment</u>

1) UDCZ is located on immediate front edge of vigorous convection.

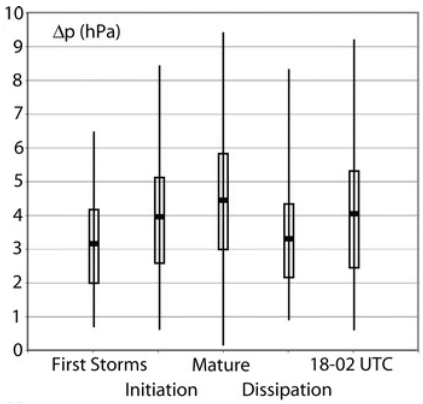

FIG. 7. E08 box and whisker plots of pressure rises (hPa) associated with analyzed cold pools for first storms, MCS initiation, mature MCS, and MCS dissipation life cycle stages, as well as for the stations that had the convective line pass overhead between 1800 and 0200 UTC. Boxes denote the 50% of values between the 25th and 75th percentiles (the interquartile range), with the thin vertical line indicating the maximum and minimum values and the horizontal line within each box indicating the mean value.

2) Radar cross-section or all-tilts displays indicate updrafts are nearly vertical and deep in nature (perhaps compared to other convection within the QLCS).
3) A strong reflectivity gradient is noted on the forward flank of the segment.
4) Echo tops may be higher than surrounding convection.
5) Trailing stratiform precipitation.

<u>Indicators of a shear dominant line segment</u>

1) Near-surface UDCZ is located behind developing updrafts.
2) Radar cross-section or all-tilts displays indicate updrafts are forward leaning with less vertical development.
3) Width of the updrafts can be notably thin.
4) Potential leading stratiform precipitation.

Overlaying 0-3 km bulk shear vectors with a 0.5° Z/SRM combination is an efficient way to diagnose the three ingredients which favor mesovortex genesis:

1) Use the Z/SRM combination to determine the location of the UDCZ and diagnose regions of balanced or slightly shear dominant regimes.
2) Compare 0-3 km bulk shear vectors to the UDCZ and determine where line-normal magnitudes are equal to or greater than 15 m s^{-1}.
3) Use the Z/SRM combination (including higher tilts) to diagnose regions where the QLCS will surge or bow out.

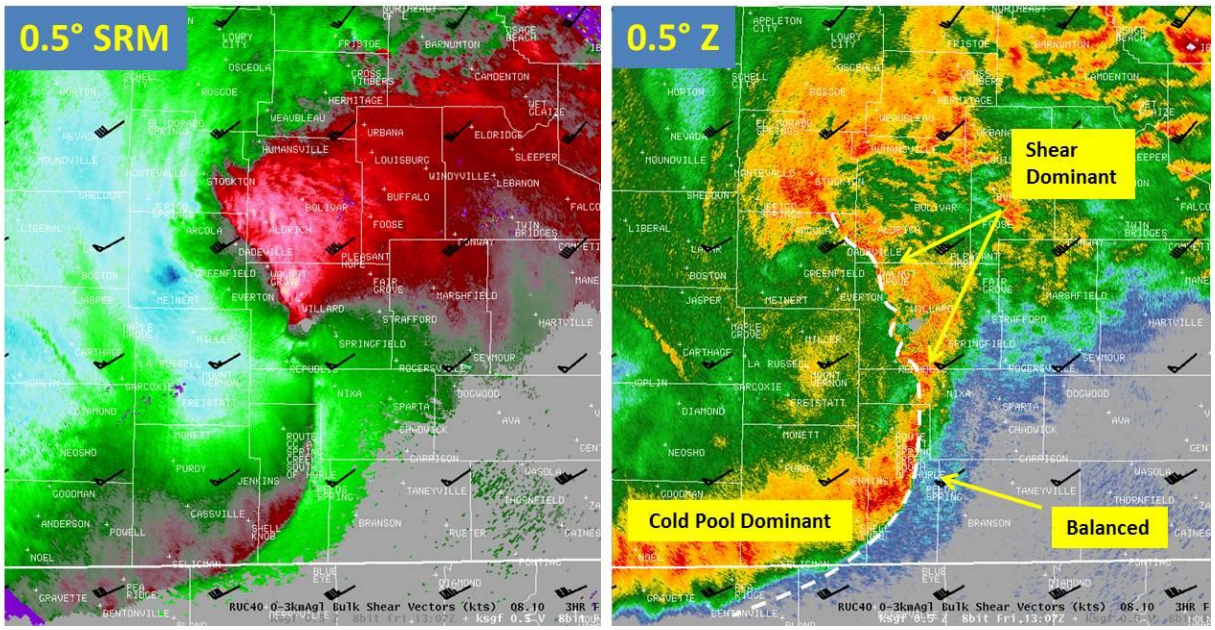

FIG. 8. These radar images depict the 8 May 2009 super-derecho as it was moving into Springfield, MO. The UDCZ is readily apparent on the 0.5° SRM image (left). Comparison of the UDCZ (dashed white line in right image) to 0.5° Z effectively highlights differing shear/cold pool balance regimes. 0-3 km bulk shear vectors (knots) are overlaid in black.

While we have observed a limited number of weaker and shorter-lived mesovortices when one or more of these ingredients were absent, our observations indicate that *the potential for mesovortex genesis and strong intensification is greatly increased when all three ingredients co-exist*.

Comparison of inferred shear and cold pool balance regimes to 0-3 km bulk shear vectors also gives radar operators a method to anticipate the evolution of a QLCS. Once cold pool conglomeration commences and a MCS begins to mature, the vast majority of MCSs will produce at least marginal cold pool pressure rises as shown by E08. Thus, some net contribution of 0-3 km bulk shear will be needed to "balance" the cold pool. If 0-3 km bulk shear vectors are parallel to the UDCZ, there will be no net contribution of 0-3 km shear and would likely result in a cold pool dominant line or line segment. In many instances, portions of a QLCS that are normal to 0-3 km bulk shear vectors will stand the best chance of remaining in a near-balanced state. Short term forecast plots of these vectors in conjunction with a radar loop can be a valuable tool to highlight areas within a QLCS which may remain in a near-balanced state for the next 1-2 hours.

One scenario where line-normal shear vectors would not promote balance would be in a strongly sheared low-level environment. Using Table 1 as an approximation of potential cold pool strength, we have observed very few instances in which cold pool pressure rises have exceeded 8 mb. Thus, magnitudes of 0-3 km line-normal bulk shear greater than 21 m s^{-1} would likely lead to a shear dominant regime. This can often be the case during the cold season. In high shear environments, one would look for an angle to the 0-3 km bulk shear vectors in relation to the UDCZ. The proper angle would effectively reduce the line-normal magnitude of bulk shear and promote balance with a system cold pool. 0-3 km bulk shear vectors for the 8 May 2009 super-derecho were orientated to the northeast at 20-26 m s^{-1} (Figures 7 and 8). In this particular case, the balanced region of this MCS featured vectors orientated about 60º to the UDCZ. Despite the 60º angle to these vectors, the line-normal magnitudes in the balanced region still exceeded 15 m s^{-1}. This system went on to spawn over 20 tornadoes across southern Missouri.

While the state of shear/cold pool balance is not an entity that can be readily forecast prior to the development of a QLCS, there are methods in which forecasters can assess the potential for mesovortex development and tornadoes ahead of time. If a MCS is forecast to develop, comparing its expected movement to 0-3 km bulk shear vectors can reveal at least the potential for line-normal magnitudes to meet or exceed the 15 m s^{-1} threshold. Forecasters may then elect to advertise tornado potential. Given a greater likelihood for a near balanced regime, forecasters could also convey the potential for a "greater straight-line wind threat" with any line segments which bow in a fashion perpendicular to the shear vectors.

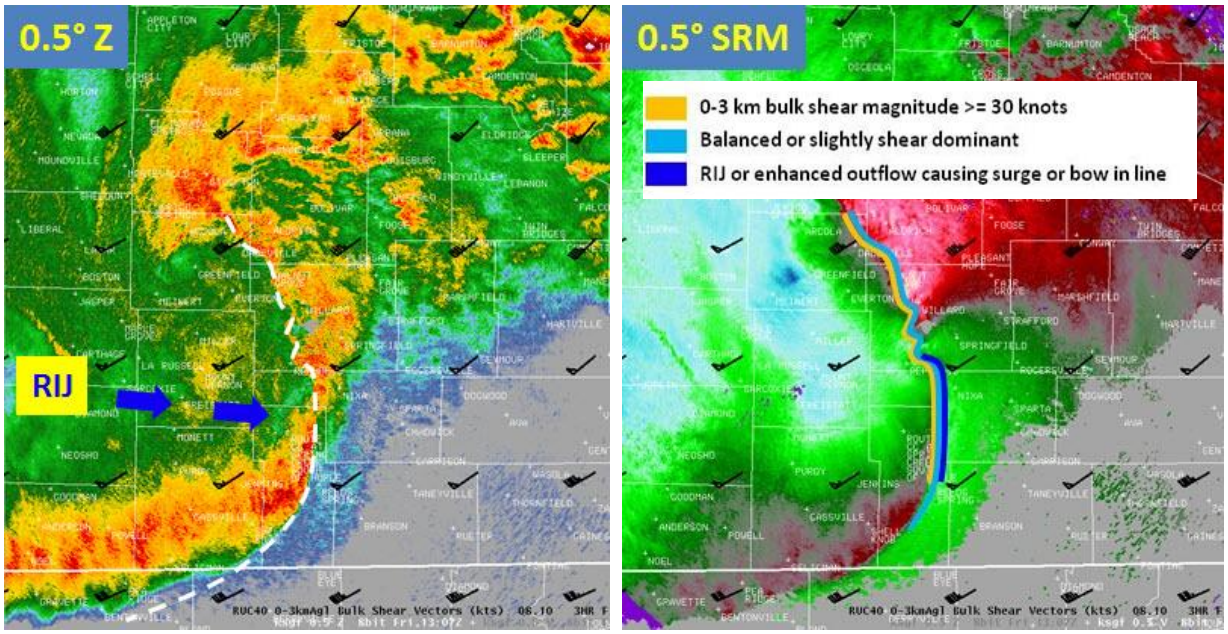

FIG. 9. These radar images of the 8 May 2009 super-derecho are valid at the same time as those in Figure 8. 0-3 km bulk shear vectors (knots) are overlaid in black. The left image depicts 0.5° Z with the location of an impinging RIJ. The UDCZ is denoted by a dashed white line. The right image then depicts 0.5° SRM and color-codes portions of the UDCZ based on the three ingredients favorable for mesovortex genesis and intensification. The light orange shading highlights areas of the QLCS where 0-3 km line-normal bulk shear magnitude was equal to or greater than 15 m s^{-1} (30 knots). The pale blue shading depicts areas of the QLCS that were balanced or slightly shear dominant. The dark blue shading highlights areas of the QLCS where a descending RIJ resulted in a bow structure in the line.

3. CASE STUDIES

a. 26-27 June 2011 Tornadic QLCS

Scattered to numerous thunderstorms developed across western and central Nebraska during the late morning and afternoon of 26 June 2011. These thunderstorms developed as an upper level trough and associated height falls overspread the region (Figure 10). At the surface, a cold front slowly moved east that afternoon and evening across the northern Plains. Meanwhile, a stationary front extended along the Interstate 70 corridor across Kansas and Missouri (Figure 11).

As cold pools conglomerated across Nebraska, a large MCS developed and strengthened across eastern Nebraska and western Iowa during the late afternoon and early evening. A pronounced line of storms then began to turn southeast and expand in areal coverage late that evening, shifting into northern Missouri starting around 0400 UTC. The line of storms produced a large swath of wind damage (not shown) from southern Iowa into northern Missouri. As the storms continued to move southeast across northern Missouri, they tended to track along the aforementioned surface front. RUC40 MUCAPE values ranged from around 1000 J kg^{-1} near the front across northern Missouri to 2500 J kg^{-1} across portions of central Missouri (Figure 12). Convective inhibition for a mean (0-1 km) parcel was rather high across the region with the RUC40 indicating values between -200 and -400 J kg^{-1} (not shown). 0-6 km bulk shear of 20-26 m s^{-1} was supportive of organized convection (Figure 13).

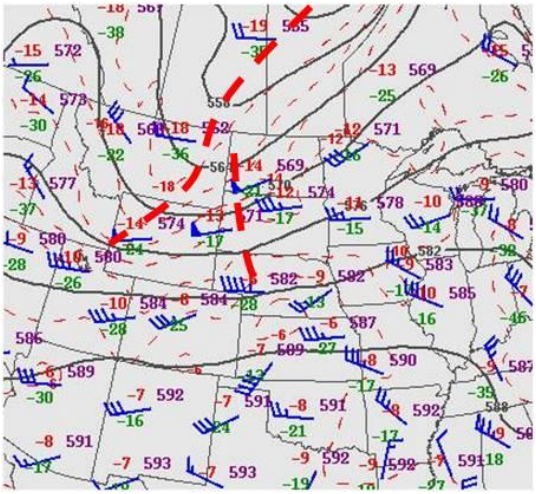

FIG. 10. 500 hPa plot valid on 27 June 2011 at 0000 UTC. Trough axes (dashed red lines) added by authors. Original plot courtesy of the Storm Prediction Center (SPC).

Bulk shear vectors within the 0-3 km layer were orientated from southwest to northeast around 18 m s^{-1} ahead of this line across northeastern and east-central Missouri (Figure 14). As this line moved through Kirksville, Missouri, a cold pool pressure rise of 6.4 mb was recorded between 0455 and 0529 UTC (not shown). Using Table 1 as an approximation, 18-19 m s^{-1} of line-normal 0-3 km bulk shear would be required to balance a cold pool of this strength. Given that 0-3 km bulk shear vectors were orientated in a non-normal fashion to the line, the line-normal magnitudes were less than 15 m s^{-1} and resulted in this MCS being outflow dominant as it tracked across north-central Missouri.

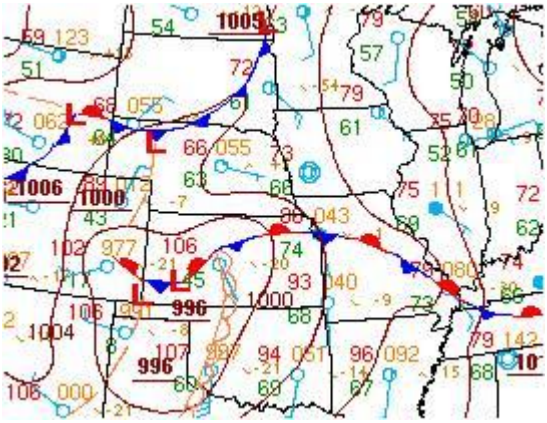

FIG. 11. Surface plot valid on 27 June 2011 at 0000 UTC. Plot courtesy of the Hydrometeorological Prediction Center (HPC).

The line then took on bowing characteristics and began to pivot more eastward across northeastern and east-central Missouri after 0500 UTC. The northern portion of the bow echo became aligned nearly normal to the 0-3 km bulk shear vectors just to the east of Macon, Missouri as a RIJ impinged on the UDCZ (Figure 15). The start of a localized surge within the larger bow echo is also evident between Macon and Shelbina. A comparison of 0.5° Z and SRM products also indicated that this portion of the line was in balance as the UDCZ was located on the immediate front edge of vigorous updrafts. This portion of the line therefore exhibited all three ingredients favorable for mesovortex genesis and strong intensification as it approached Shelbyville and Shelbina.

1) The UDCZ was located directly downshear of vigorous updrafts indicating balance between the system cold pool and ambient shear.
2) Line-normal bulk shear magnitudes were 17-19 m s^{-1}.
3) An impinging RIJ resulted in a bowing structure. A localized surge within the bow echo also occurred.

One tornado developed and tracked east-southeast through the town of Shelbina. A second tornado developed in the extreme southern portion of Shelbina and also tracked southeast (Figure 16). Two additional tornadoes occurred about 15 miles to the east-southeast of Shelbina (tracks not shown).

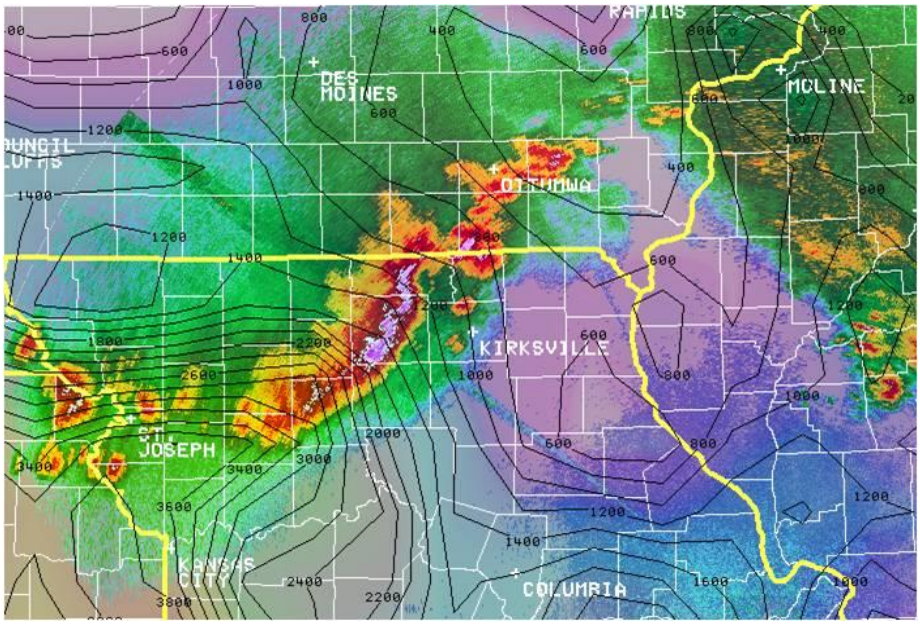

FIG. 12. KLSX 0.5° Z image valid on 27 June 2011 at 0452 UTC. RUC40 MUCAPE (J kg^{-1}) is depicted by black contours.

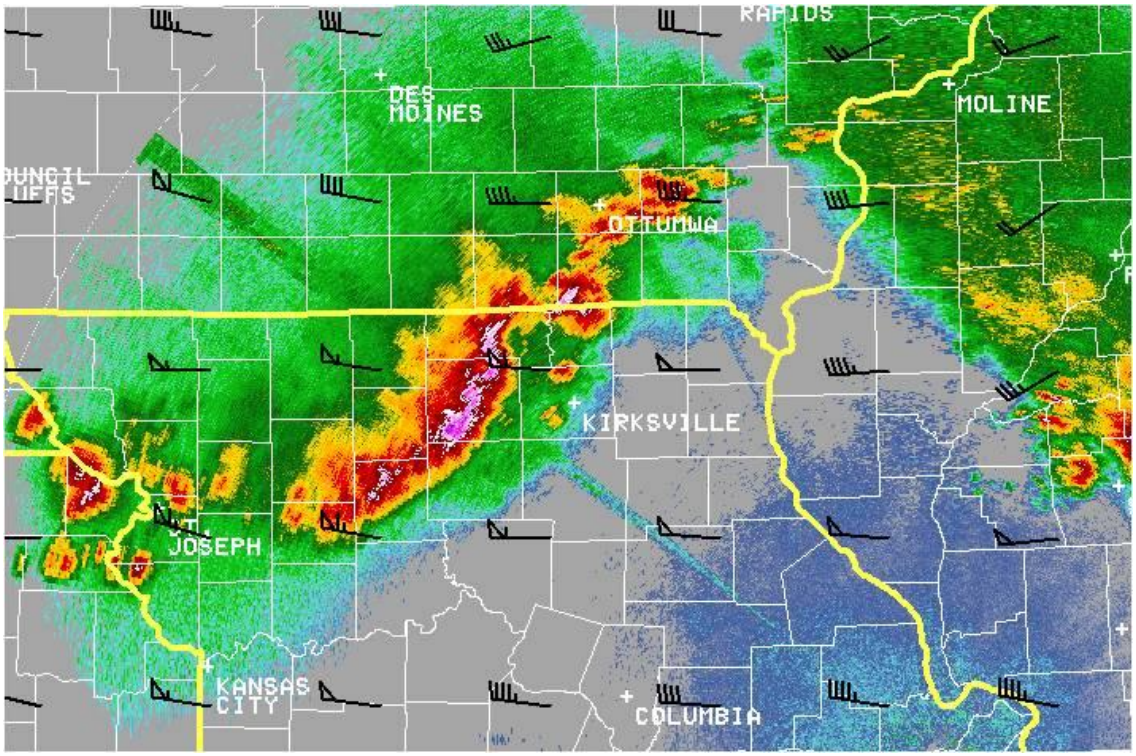

FIG. 13. KLSX 0.5° Z image valid on 27 June 2011 at 0452 UTC. RUC40 0-6 km bulk shear vectors (knots) overlaid in black.

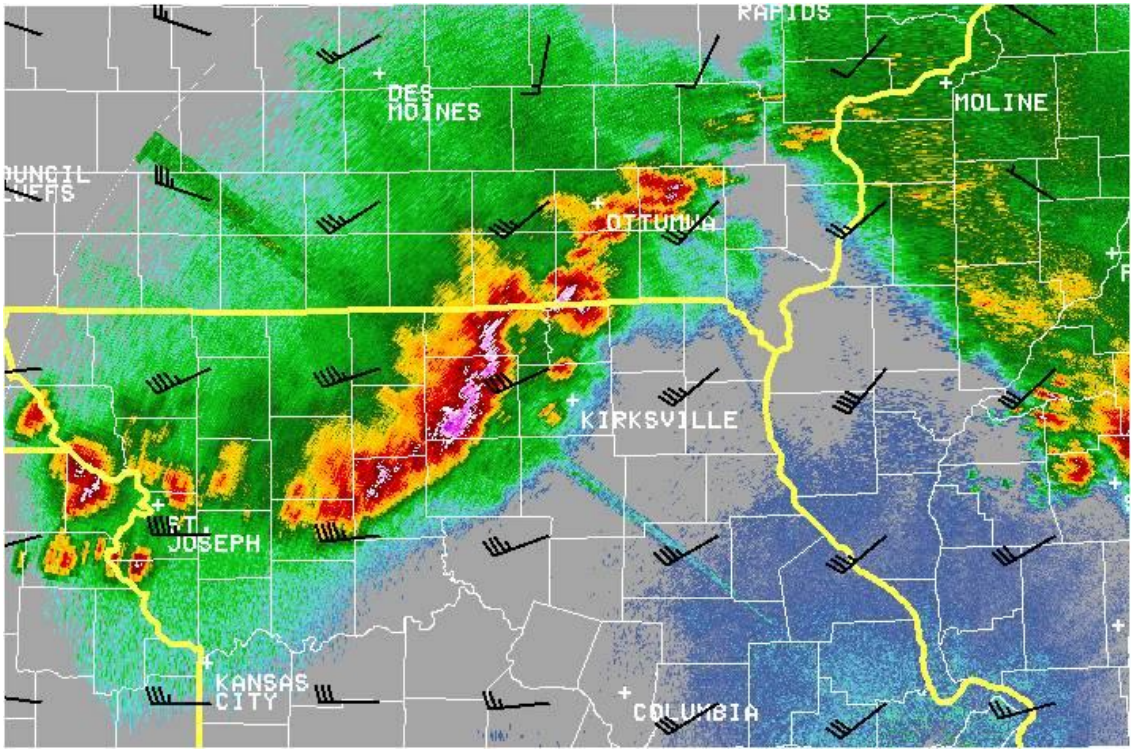

FIG. 14. KLSX 0.5° Z image valid on 27 June 2011 at 0452 UTC. RUC40 0-3 km bulk shear vectors (knots) overlaid in black.

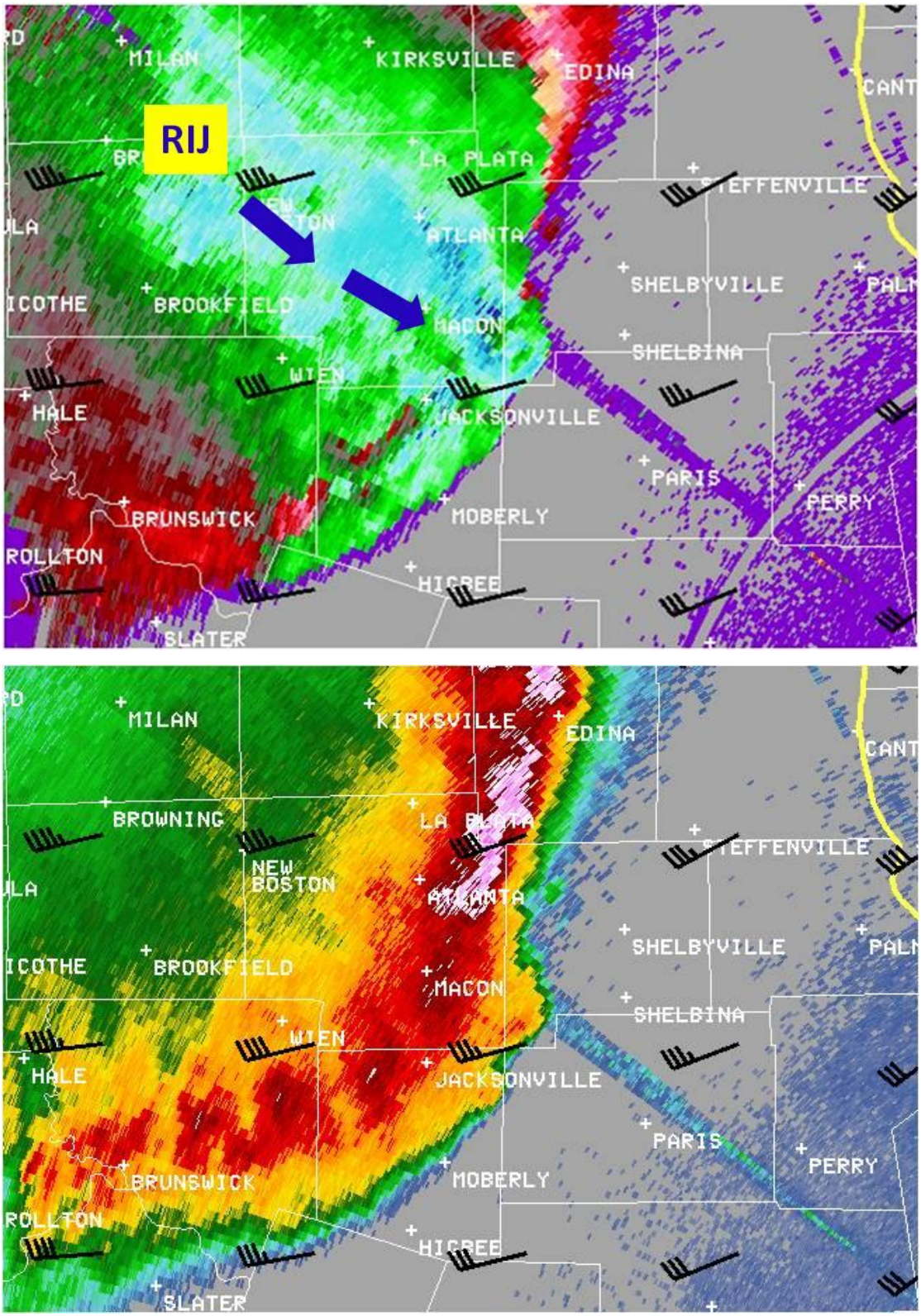

FIG. 15. KLSX 0.5° SRM/Z images valid on 27 June 2011 at 0537 UTC. RUC40 0-3 km bulk shear vectors (knots) overlaid in black. A RIJ is structure is present on the SRM product with the 0.5° beam height between 12 and 13 kft AGL.

FIG. 16. A damage assessment conducted by the National Weather Service in St. Louis, Missouri revealed that two EF-1 tornadoes occurred in Shelbina, Missouri.

b. 18-19 June 2011 Tornadic QLCS

The synoptic scale pattern during the late afternoon and early evening hours of 18 June 2009 featured a short wave trough tracking east across the central Plains (Figure 17). A 20-25 m s^{-1} 850 hPa low-level jet developed during the early evening hours from eastern Texas and nosed into western Missouri (not shown). Weak surface low pressure was located across central Oklahoma, with a stationary surface front extending northeast from the low into west-central Missouri (Figure 18).

The environment across western Missouri featured large amounts of instability with the 0000 UTC KSGF RAOB indicating MLCAPE values well over 4000 J kg^{-1} (Figure 19). This RAOB also revealed theta-e differentials around 40 Kelvin (K) between the surface and about 700 hPa, which favored strong cold pool potential. 0-6 km bulk shear of 18-22 m s^{-1} was supportive of organized convection across the region (not shown).

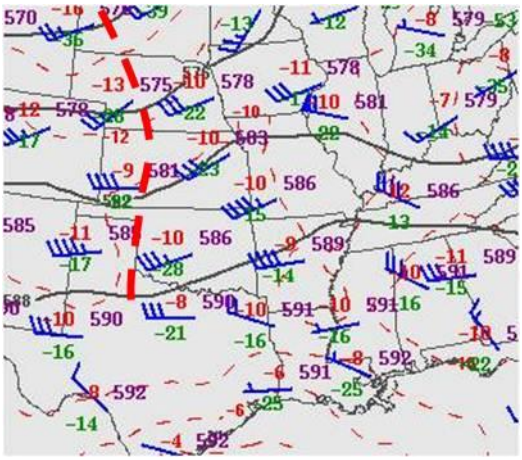

FIG.17. 500 hPa plot valid on 19 June 2011 at 0000 UTC. Trough axis (dashed red line) added by authors. Original plot courtesy of SPC.

Scattered thunderstorms initially developed across extreme southeastern Kansas during the late afternoon hours and expanded in areal coverage that evening as the low-level jet increased and overrode the surface front. Several of these storms initially took on

supercellular characteristics with several reports of large hail.

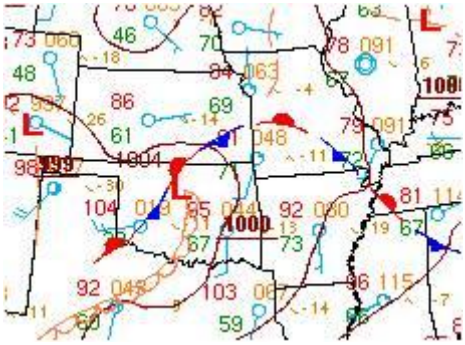

FIG. 18. Surface plot valid on 19 June 2011 at 0000 UTC. Plot courtesy of HPC.

These storms began to congeal into a MCS by 0300 UTC as cold pools began to conglomerate. By this time, modification of the 0000 UTC KSGF RAOB and RUC data indicated MUCAPE values of around 3000 J kg^{-1} extending east from this developing MCS into portions of central and southern Missouri (not shown). Convective inhibition for a mean parcel ranged from -50 to -100 J kg^{-1} (not shown). The large values of CAPE and theta-e differentials over 30 K indicated a strong likelihood for a forward propagating MCS where the mean flow was perpendicular to the gust front (Corfidi 2003). Forward propagating Corfidi vectors (Figure 20) across central and southern Missouri were orientated from west to east at 17-24 m s^{-1}.

Bulk shear vectors in the 0-3 km layer were orientated from 250-270° at 15-18 m s^{-1} (Figures 20 and 21). Thus, bulk shear magnitudes for portions of the MCS orientated nearly normal to these vectors would support increased mesovortex and tornado potential. Interestingly, the orientation of forward propagating Corfidi vectors and 0-3 km bulk shear vectors were very similar for this case (Figure 20). Thus, it was feasible to assume that some portion of a forward propagating MCS would be normal to the 0-3 km bulk shear vectors.

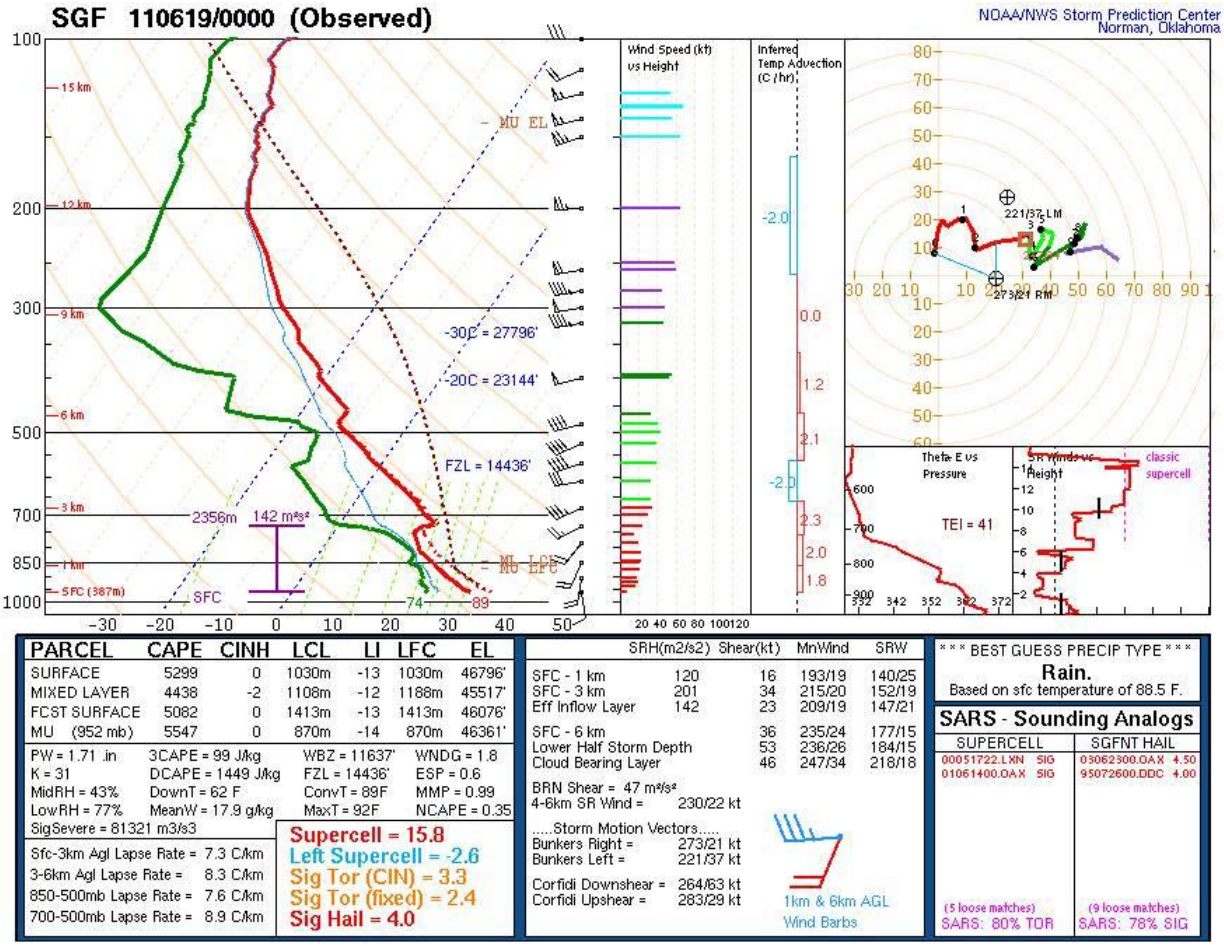

FIG. 19. KSGF RAOB valid on 19 June 2011 at 0000 UTC. Image courtesy of SPC.

By 0400 UTC, this relatively compact MCS began to accelerate eastward across southwestern Missouri (Figure 21). Inspection of radar data showed a maturing RIJ structure to the northwest of Springfield (not shown). The MCS began to bow out at this point with inbound radial velocities approaching 40 m s^{-1} (not shown). During the surging stages of the bow, it was readily apparent that the bowing section of the MCS just to the east of Greenfield, Missouri contained all three ingredients favorable for mesovortex genesis and strong intensification.

1) The UDCZ was located directly downshear of vigorous updrafts, indicating balance between the system cold pool and ambient shear.
2) Line-normal bulk shear magnitudes were 15 m s^{-1}.
3) An impinging RIJ resulted in a bowing structure.

In contrast, southern portions of the convective line were cold pool dominant as the convective outflow was clearly outrunning the main convection. 0-3 km bulk shear vectors were orientated nearly parallel to the convection around Miller, Missouri, resulting in line-normal magnitudes of only 8 m s^{-1}.

This system spawned three tornadoes to the north and northwest of Springfield between 0400 and 0600 UTC (Figure 22), and would produce two additional tornadoes in Crawford County, Missouri later that night (not shown). Several reports of straight-line wind damage were also received along the track of the advancing bow structure.

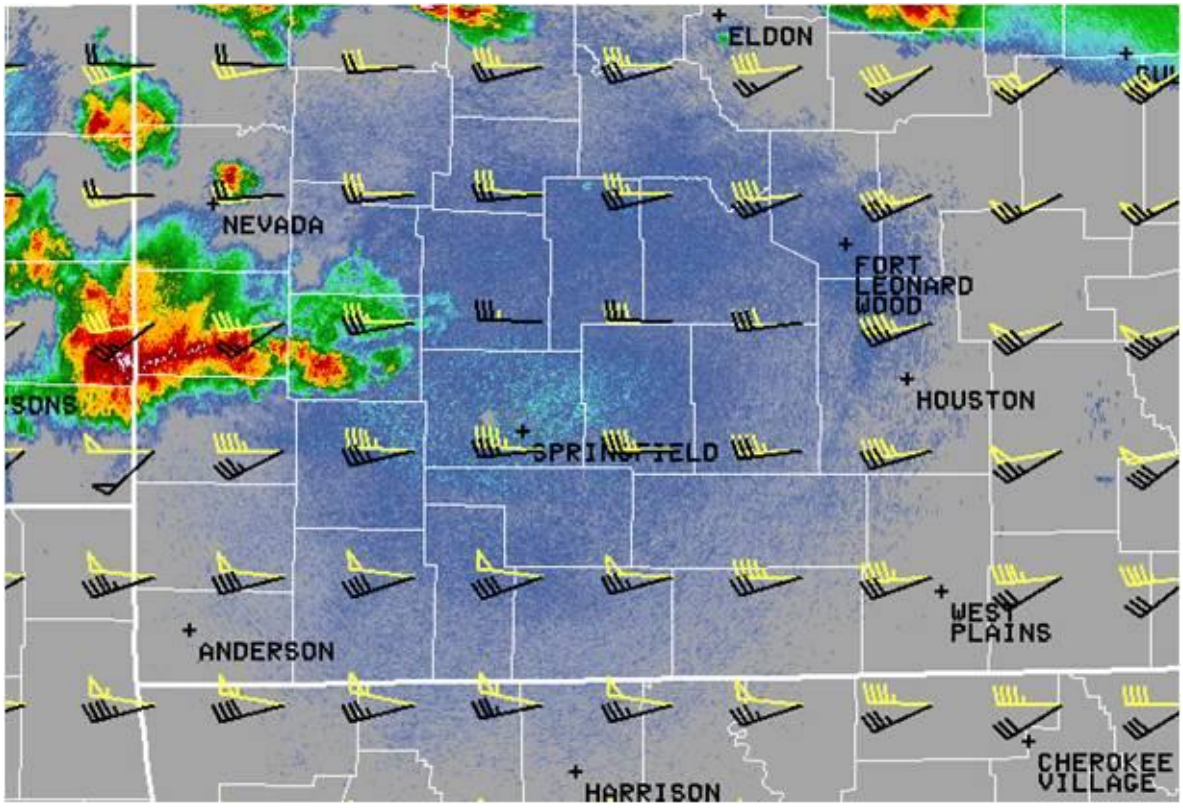

FIG. 20. KSGF 0.5° Z image valid on 19 June 2011 at 0349 UTC. RUC40 forward propagating Corfidi vectors (knots) are overlaid in yellow while RUC40 0-3 km bulk shear vectors (knots) are overlaid in black.

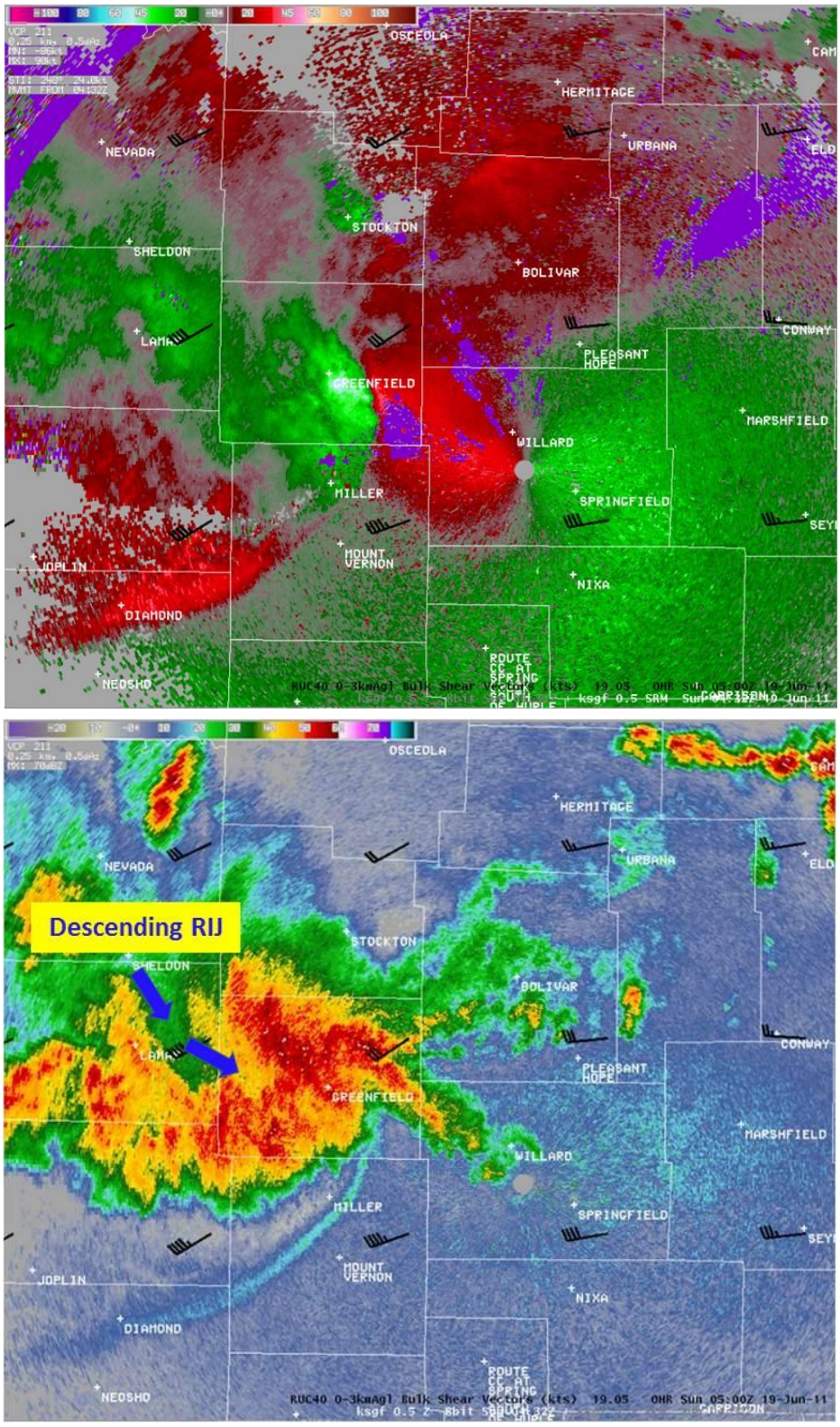

FIG. 21. KSGF 0.5° SRM/Z images valid on 19 June 2011 at 0432 UTC. RUC40 0-3km bulk shear vectors (knots) are overlaid in black. A descending RIJ resulted in a bowing line segment near Greenfield, Missouri.

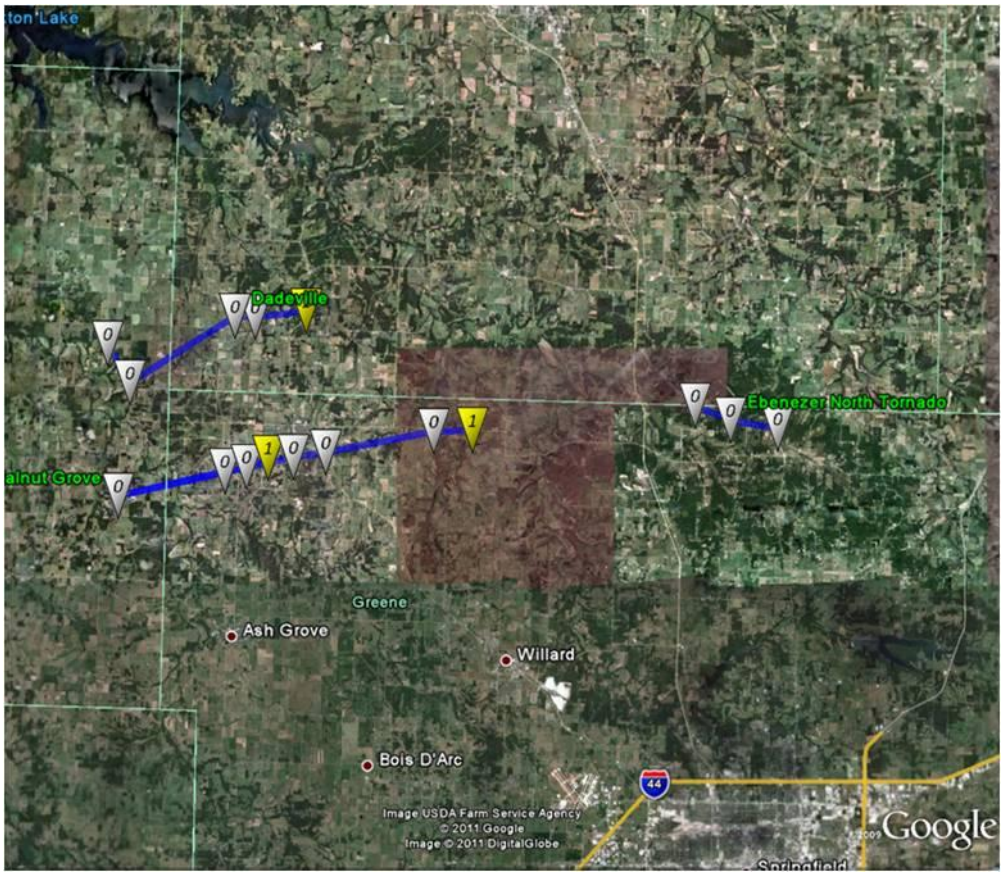

FIG. 22. A damage assessment conducted by the National Weather Service in Springfield, Missouri revealed that three tornadoes occurred between 0400 and 0600 UTC just to the north and northwest of Springfield, Missouri.

c. 19 July 2006 St. Louis Derecho

The synoptic scale environment on 19 July 2006 featured a sprawling upper level ridge centered over the central United States (Figure 23). A MCS was ongoing early that morning across southern Minnesota where theta-e advection was maximized on the nose of a low-level jet (not shown). At 1500 UTC, a warm front was analyzed from extreme northern Nebraska, southeast into southern Illinois (Figure 24). 1200 UTC RAOBs along and south of the frontal boundary were representative of a very unstable air mass with strong cold pool potential. Inspection of the 1200 UTC KILX RAOB revealed theta-e-rich air just off the surface with nearly dry adiabatic lapse rates above a capping inversion (Figure 25). Of particular note is the rapid decreased in relative humidity between 850 and 800 hPa.

By 1800 UTC, the eastern portion of the warm front had lifted north and was located in northern Illinois (not shown). The MCS maintained an east-southeast track into eastern Iowa and generally remained north of the frontal boundary (not shown). By mid afternoon, the MCS turned nearly due south and crossed the surface front as it tracked along the periphery of the upper level ridge. The atmosphere to the south of this system had become very unstable with surface temperatures well

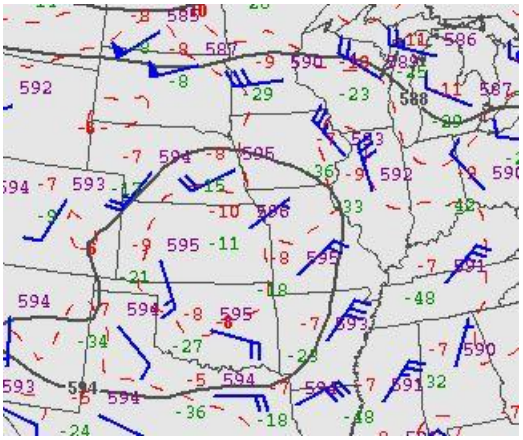

FIG. 23. 500 hPa plot valid on 19 July 2006 at 1200 UTC. Plot courtesy of SPC.

into the 90s and dew points in the middle 70s (not shown). The 2100 UTC RUC40 indicated MUCAPE values of 4000-7000 J kg^{-1} ahead of the southward moving line across east-central Missouri and central Illinois (Figure 26), with convective inhibition ranging from -25 to -75 J kg^{-1} (not shown). Theta-e differentials from the 2100 UTC RUC were extreme with values generally exceeding 40 K (Figure 27). These values supported strong cold pool development. Interestingly, 0-6 km bulk shear values ahead of the line were somewhat modest with values of 12-16 m s^{-1} (Figure 28). This may have resulted in the convection becoming less organized in nature by late afternoon.

As this line approached the St. Louis metropolitan area, a comparison of SRM and Z products revealed that the system was cold pool dominant as the gust front was located ahead of the main convection (Figure 29). As the MCS moved through the St. Louis area, cold pool pressure rises of around 6 mb were recorded. Referring back to Table 1, it would take line-normal 0-3 km bulk shear values of around 18 m s^{-1} to balance this cold pool. While the RUC40 indicated that 0-3 km bulk shear vectors were orientated nearly normal to this portion of the line, magnitudes were only around 8 m s^{-1} (Figure 29).

While enough constructive interference from the interaction of the system cold pool and environmental shear was in place to force parcels over the LFC and maintain the MCS, this system did not exhibit the three ingredients which favored mesovortex genesis and strong intensification.

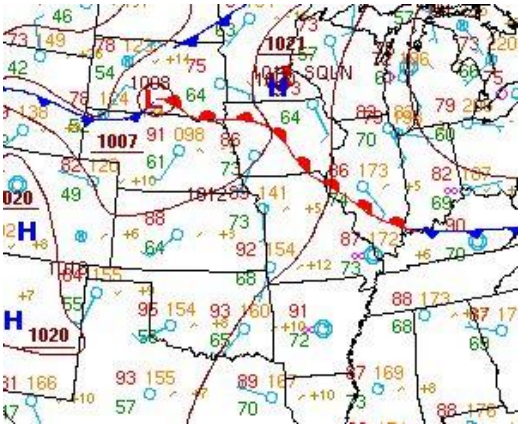

FIG. 24. Surface plot valid on 19 July 2006 at 1500 UTC. Plot courtesy of HPC.

1) The line was not in balance.
2) 0-3 km line-normal bulk shear magnitudes were less than 15 m s^{-1}.
3) A bowing structure was not present due to modest deep-layer shear.

As this system moved into St. Louis, 0.5° radial velocities exceeded 30 m s^{-1} (Figure 30). This system produced a wide swath of significant straight-line wind

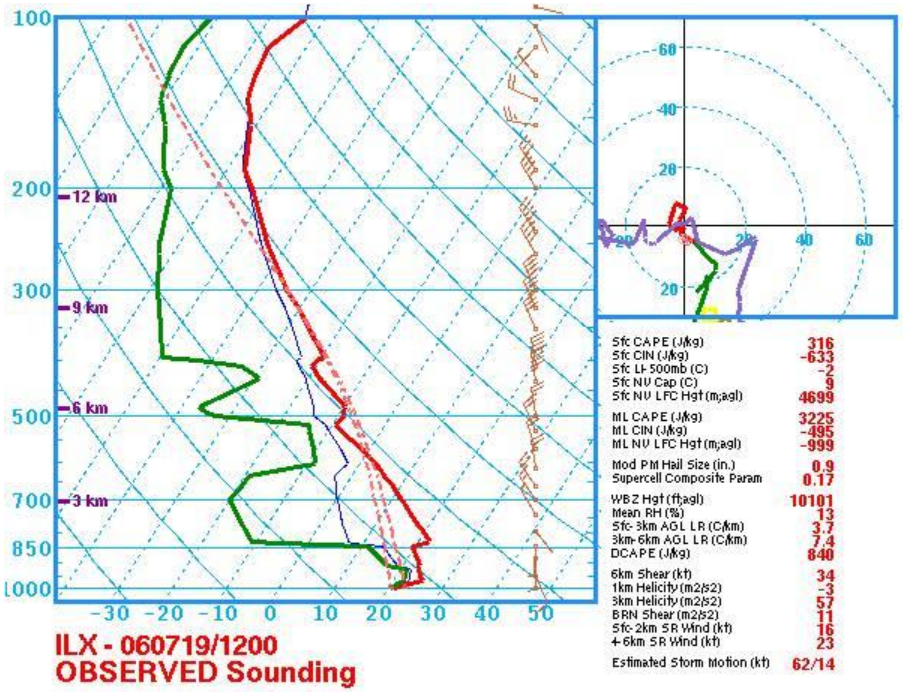

FIG. 25. KILX RAOB valid on 19 July 2006 at 1200 UTC. Image courtesy of SPC.

damage from eastern Iowa through western Illinois and eastern Missouri. The damage sustained in the St. Louis metropolitan area was consistent with wind speeds of 31-36 m s^{-1}. Areas of damage across western Illinois suggested that wind speeds could have approached 40 m s^{-1}. While nearly all of the structural and tree damage was caused by intense downburst clusters and microbursts, storm surveys conducted by the National Weather Service in St. Louis, Missouri revealed two brief and weak F-0 tornadoes occurred near Bunker Hill and Edwardsville in southwestern Illinois (Figure 31). Inspection of radar data indicates that these tornadoes likely occurred under areas of intense convective updrafts in an environment supportive of rapid upward parcel acceleration. The tornadoes also occurred where the gust front was in closer proximity to developing updrafts. Although still cold pool dominant, this portion of the MCS realized the maximum contribution of low-level shear as 0-3 km bulk shear vectors were orientated normal to the line. In contrast, the gust front was located further downstream from developing updrafts along the western extent of the line. For additional details on this case, see Przybylinski et al. (2008).

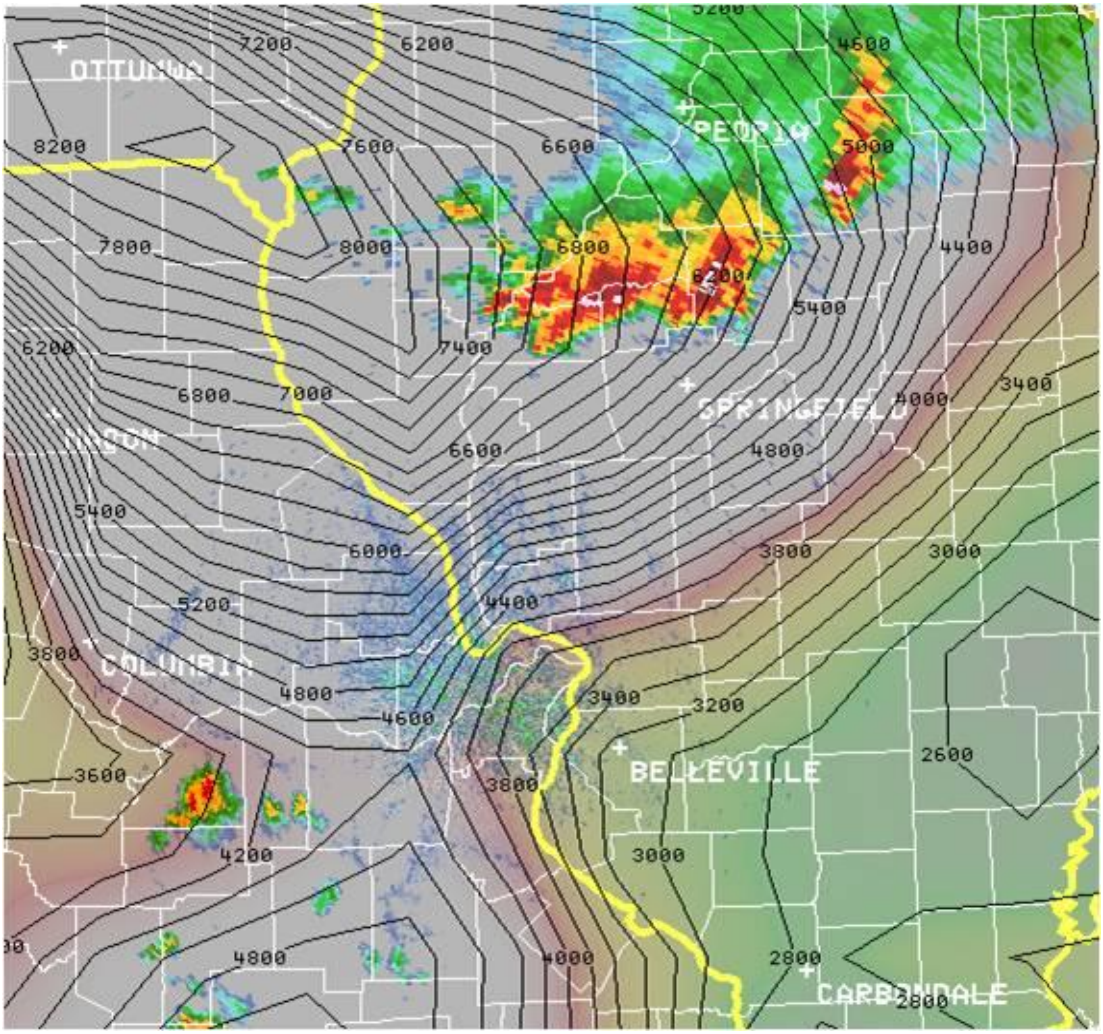

FIG. 26. KLSX 0.5° Z image valid on 19 July 2006 at 2159 UTC. RUC40 MUCAPE (J kg^{-1}) is depicted by black contours.

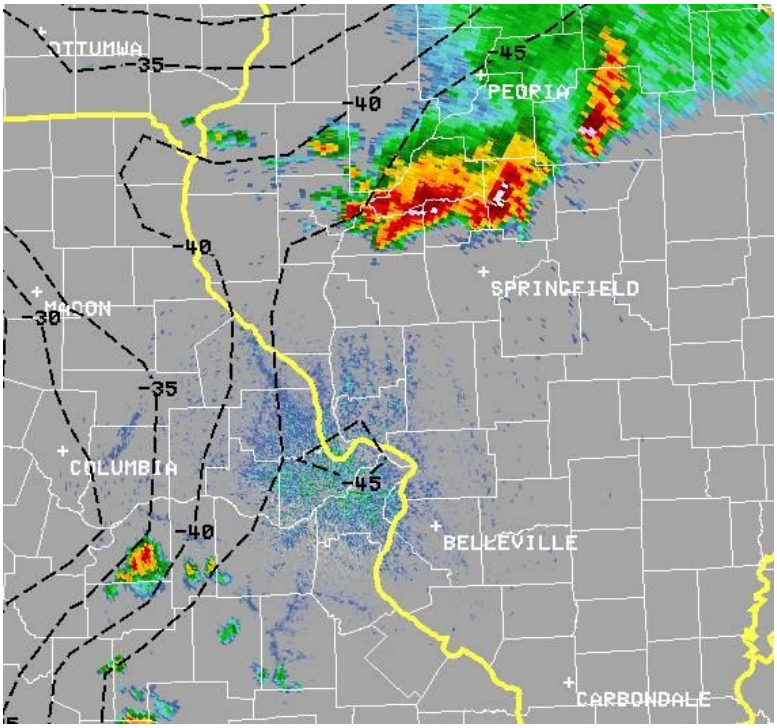

FIG. 27. KLSX 0.5° Z image valid on 19 July 2006 at 2159 UTC. RUC40 0-3 km maximum theta-e differential (K) is depicted by black contours.

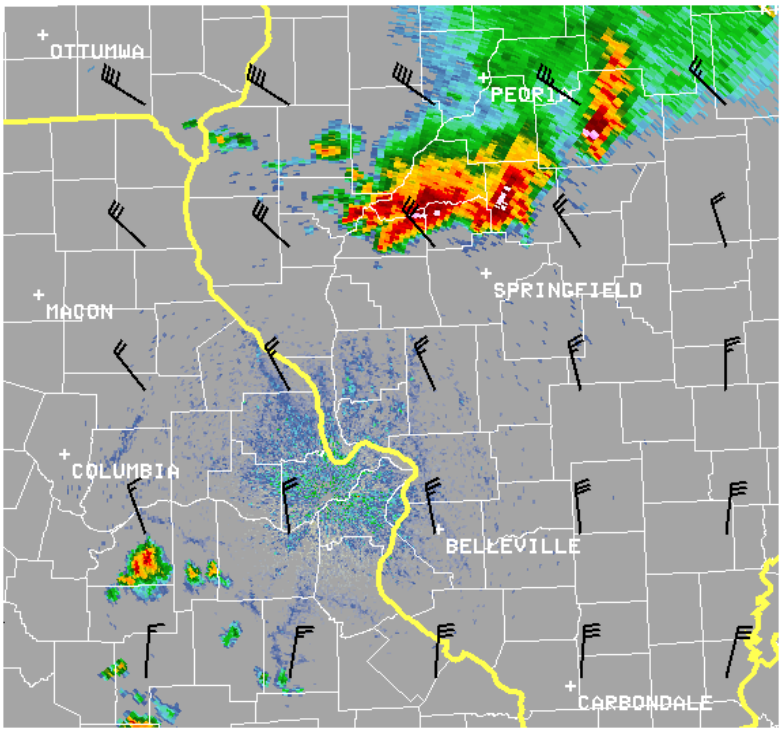

FIG. 28. KLSX 0.5° Z image valid on 19 July 2006 at 2159 UTC. RUC40 0-6 km bulk shear vectors (knots) overlaid in black.

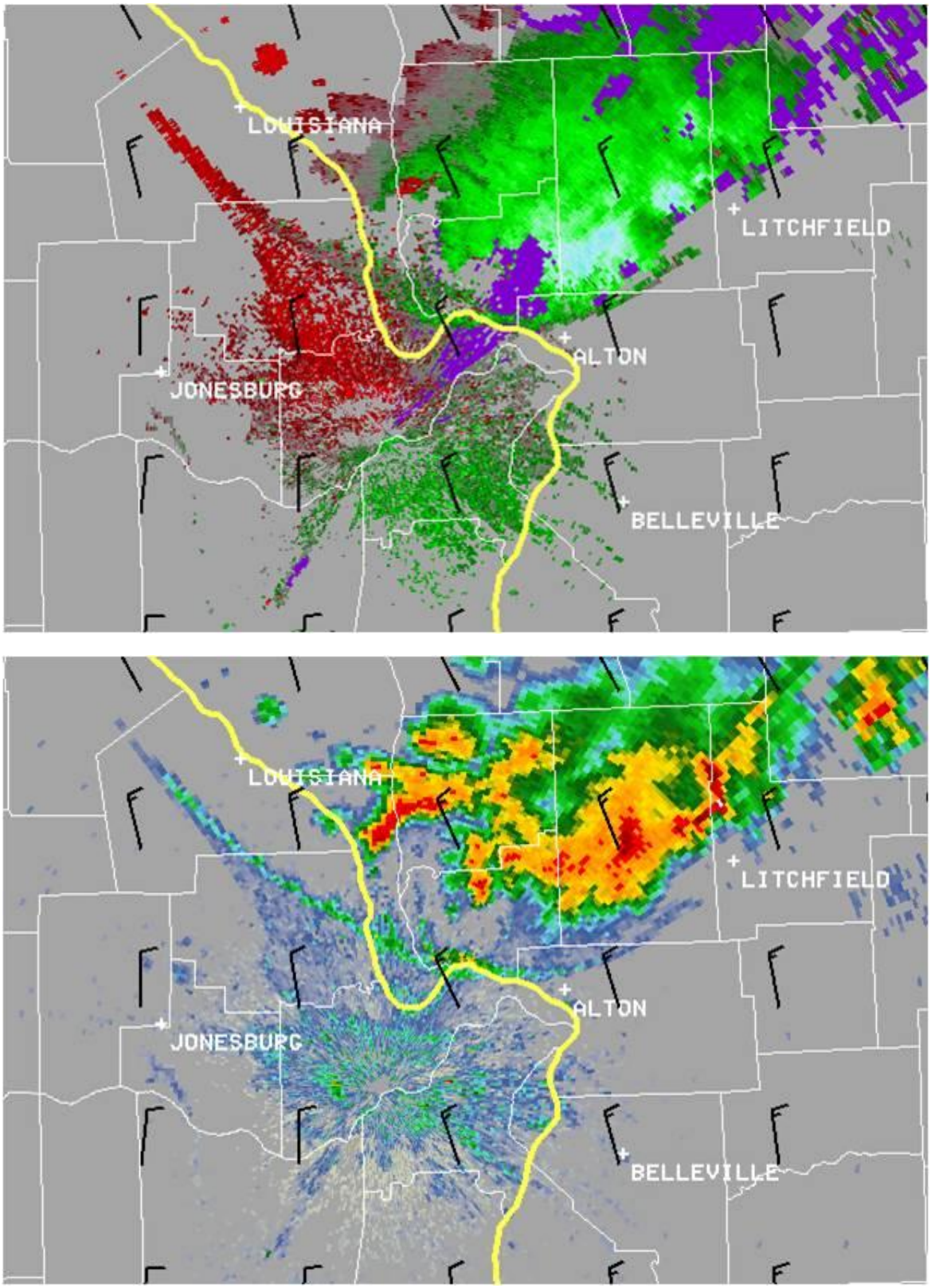

FIG. 29. KLSX 0.5° SRM/Z images valid on 19 July 2006 at 2332 UTC. RUC40 0-3 km bulk shear vectors (knots) overlaid in black.

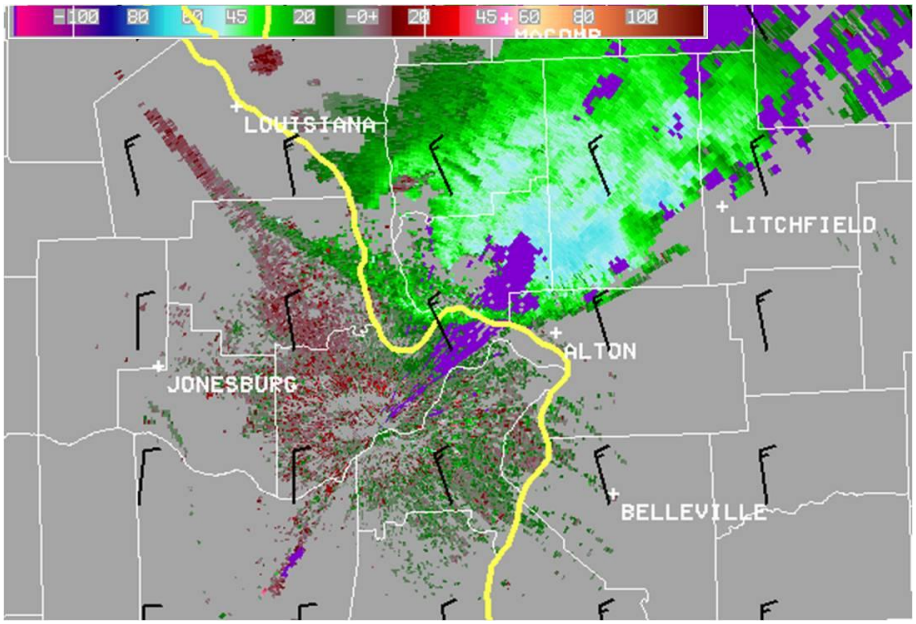

FIG. 30. KLSX 0.5° radial velocity image valid on 19 July 2006 at 2332 UTC. RUC40 0-3 km bulk shear vectors (knots) overlaid in black.

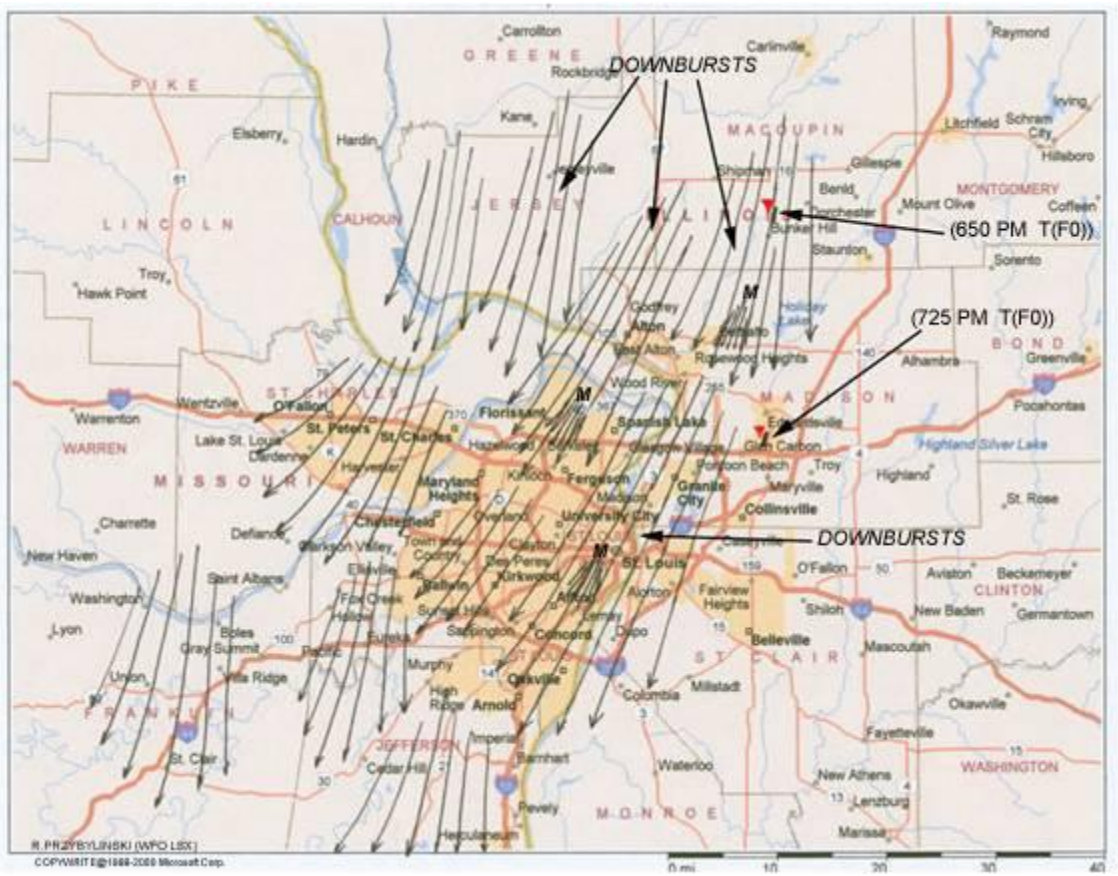

FIG. 31. A damage assessment conducted by the National Weather Service in St. Louis, Missouri revealed extensive straight-line wind damage in the St. Louis metropolitan area. Two brief F-0 tornadoes also occurred to the northeast and east of St. Louis.

4. SUMMARY

Close examination of several progressive MCSs has yielded three co-existing criteria which correlate to a greater likelihood for mesovortex genesis and subsequent intensification, along with increased tornado potential. The likelihood for tornado-producing mesovortices increases:

1) In a portion of a QLCS in which the cold pool and ambient low-level shear are nearly balanced or slightly shear-dominant ***AND***
2) Where 0-3 km line-normal bulk shear magnitudes are equal to or greater than 15 m s^{-1} (30 knots) ***AND***
3) Where a RIJ or enhanced outflow causes a surge or bow in the line.

Identification of QLCS regions favorable for mesovortex development and intensification may promote increased lead time and detection for QLCS tornadoes. Given that this methodology would also highlight areas within a QLCS less favorable for mesovortex genesis and intensification, it is reasonable to assume that false alarm for QLCS Tornado Warnings may also be reduced.

We showed that the use of 0-3 km bulk shear vectors in conjunction with radar imagery provides radar operators with an efficient means of diagnosing the potential for mesovortex development and intensification. Comparison of low-level SRM and Z products provides valuable clues to the state of shear and cold pool balance, as well as the presence of line surges or bow echoes. Additionally, overlaying 0-3 km bulk shear vectors with Z/SRM products readily highlights portions of the UDCZ where line-normal magnitudes are equal to or greater than 15 m s^{-1}.

We also presented an alternative method of determining shear and cold pool balance through the comparison of cold pool pressure rises to 0-3 km bulk shear magnitudes. Methods of anticipating mesovortex potential in advance were also examined by comparing 0-3 km bulk shear vectors to the expected motion of QLCSs. The methods described in this paper were then applied to three case studies, each of which produced tornadoes. Additional cases are also presented at the following link:

http://www.crh.noaa.gov/sgf/?n=0-3vect_paper

Future work is planned in assessing the statistical significance of the three criteria favorable for mesovortex genesis and intensification. This research will include the examination of numerous additional MCS cases across the central and eastern United States.

5. ACKNOWLEDGEMENTS

The authors extend their gratitude to Mr. Ken Cook (SOO WFO ICT) for sharing his cold pool strength table. Additional thanks goes John Gagan and Andy Boxell (WFO Springfield, MO), as well as Dr. Nolan Atkins (Lyndon State College) for their constructive comments on improving the paper. We also thank Ms. Melinda Schaumann for her assistance in the construction and layout of the accompanying poster. Finally, we thank Mr. William Davis (MIC WFO Springfield, MO) and Mr. Wes Browning (MIC WFO St. Louis, MO) for their administrative support.

6. REFERENCES

Atkins, N.T., J. M. Arnott, R. W. Przybylinski, R. A. Wolf, and B. D. Ketcham, 2004: Vortex structure and evolution within bow echoes. Part I: Single-Doppler and damage analysis of the 29 June 1998 derecho. Mon. Wea. Rev., 132, 2224–2242.

_____, C. S. Bouchard, R. W. Przybylinski, R. J. Trapp, and G. Schmocker, 2005: Damaging surface wind mechanism within the 10 June 2003 Saint Louis bow echo during BAMEX. Mon. Wea. Rev., 133, 2275–2296.

_____, and M. St. Laurent, 2009a: Bow Echo Mesovortices. Part I: Processes That Influence Their Damaging Potential. Mon. Wea. Rev., 137, 1497–1513.

_____, and M. St. Laurent, 2009b: Bow Echo Mesovortices. Part II: Their Genesis. Mon. Wea. Rev., 137, 1514–1532.

Bryan, G. H., D. Ahijevych, C. Davis, S. Trier, and M. Weisman, 2005: Observations of cold pool properties in mesoscale convective systems during BAMEX. Preprints, *11th Conf. on Mesoscale Processes,* Albuquerque, NM, Amer. Meteor. Soc., JP5J.12.

Burgess, D. W., 1974: Study of a right moving thunderstorm utilizing new single Doppler radar evidence. Masters Thesis, Dept. of Meteor., University of Oklahoma, Norman, OK, 77 pp.

_____, and B. F. Smull, 1990: Doppler radar observations of a bow echo with a long-track severe windstorm. Preprints, *16th Conf. on Severe Local Storms*, Kananaskis Park, AB, Canada, Amer. Meteor. Soc., 203-208.

Cohen, A. E., M. C. Coniglio, S. F. Corfidi, and S. J. Corfidi, 2007: Discrimination of mesoscale convective system environments using sounding observations. *Wea. Forecasting*, **22**, 1045-1062.

Corfidi, S. F., 2003: Cold Pools and MCS Propagation: Forecasting the Motion of Downwind-Developing MCSs. Wea. Forecasting, 18, 997–1017.

Davies, J. M., 2006a: Tornadoes in environments with small helicity and/or high LCL heights. Wea. Forecasting, 20, 579-594.

DeWald, V. L. and T. W. Funk, 2000: WSR-88D reflectivity and velocity trends of a damaging squall line event on 20 April 1996 over south-central Indiana and central Kentucky. Preprints, *20th Conf. of Severe Local Storms,* Orlando, FL, Amer. Meteor. Soc., 177-180.

Doswell, C. A. III, 2000: "*A Primer on Vorticity for Application in Supercells and Tornadoes*". Cooperative Institute for Mesoscale Meteorological Studies, Norman, Oklahoma.

Engerer, N. A., D. J. Stensrud, and M. C. Coniglio, 2008: Surface characteristics of observed cold pools. Mon. Wea. Rev., 136, 4839–4849.

Forbes, G.S., and R.M. Wakimoto, 1983: A concentrated outbreak of tornadoes, downbursts and microbursts, and implications regarding vortex classification. *Mon. Wea. Rev.,* 111, 220-235.

Fujita, T. T., 1978: Manual of downburst identification for project NIMROD. Satellite and Mesometeorology Res. Pap. No. 156, University of Chicago, Dept. of Geophysical Sciences, pp. 104.

_____, and R. M. Wakimoto, 1981: Five scales of airflow associated with a series of downbursts on 16 July 1980. *Mon. Wea. Rev.*,**109**, 1438-1456.

Funk, T. W., K. E. Darmofal, J. D. Kirkpatrick, V. L. DeWald, R. W. Przybylinski, G. K. Schmocker, and Y.-J. Lin, 1999: Storm reflectivity and mesocyclone evolution associated with the 15 April 1994 squall line over Kentucky and southern Indiana. Wea. Forecasting, 14, 976–993.

Houze, R. A., Jr., S.A. Rutledge, M. I. Biggerstaff and B. F. Smull, 1989: Interpretation of Doppler weather radar displays of midlatitude mesoscale convective systems. *Bull. Amer. Meteor. Soc*., **70**, 608-619.

Johns, R. H., and W. D. Hirt, 1987: Derechos: widespread convectively induced windstorms. *Wea. Forecasting*, **2**, 32-49.

Jorgensen, D. P., and B. F. Smull, 1993: Mesovortex circulations seen by airborne Doppler radar within a bow-echo mesoscale convective system. *Bull. Amer. Meteor. Soc*., **74**, 2146-2157.

Markowski, P. M., Y. Richardson, E. Rasmussen, J. Straka, R. Davies-Jones, and R. J. Trapp, 2008: Vortex lines within low-level mesocyclones obtained from pseudo-dual-Doppler radar observations. *Mon. Wea. Rev.*, **136**, 3513–3535.

Przybylinski, R. W., 1995: The bow echo: Observations, numerical simulations, and severe weather detection methods. *Wea. Forecasting*, **10**, 203-218.

_____, Y.-J, Lin, G.K. Schmocker, and T.J. Shea, 1995: The use of real-time WSR-88D, profiler, and conventional data sets in forecasting a northeastward moving derecho over eastern Missouri and central Illinois. *Preprints, 14th Conf. on Wea. Analysis and Forecasting*, Dallas, Amer. Meteor. Soc., 335-342.

_____, Y.-J. Lin, C. A. Doswell III, G. K. Schmocker, T. J. Shea, T. W. Funk, K. E. Darmofal, J. D. Kirkpatrick, and M. T. Shields, 1996: Storm reflectivity and mesocyclone evolution associated with the 15 April 1994 derecho, Part I: Storm structure and evolution over Missouri and Illinois. Preprints, *18th Conf. on Severe Local Storms,* San Francisco, CA, Amer. Meteor. Soc., 509–515.

_____, G.K. Schmocker, and Y.J. Lin, 2000: A Study of Storm and Vortex Morphology during the 'Intensifying Stage' of Severe Wind Mesoscale Convective Systems. Preprints, *20th Conf. on Severe Local Storms,* Orlando FL. Amer. Meteoro. Soc. 173-176.

_____, J.E. Sieveking, B.D. Sipprell, and J.L. Guyer, 2008: The 19 July 2006 Midwest Derecho: A Meteorological Perspective and Lessons Learned. Preprints, 24th Conf. Severe Local Storms, Savannah GA, 6.4.

Rasmussen, E. N., 2003: Refined supercell and tornado forecast parameters. Wea. Forecasting, 18, 530-535.

Rotunno, R.J., J. B. Klemp, and M. L. Weisman, 1988: A theory for strong, long-lived squall lines. *J. Atmos. Sci.*, **45**, 463-485.

Schmidt, J.M., and W. R. Cotton, 1989: A High Plains squall line associated with severe surface winds. *J. Atmos. Sci.*, **46**, No. 3, 281-302.

Schmocker, G. K., R. W. Przybylinski, and Y. J. Lin, 1996: Forecasting the initial onset of damaging downburst winds associated with a Mesoscale Convective System (MCS) using the Mid-Altitude Radial Convergence (MARC) signature. *Preprints, 15th Conf. On Weather Analysis and Forecasting*, Norfolk VA, Amer. Meteor. Soc., 306-311.

Thompson, R. L., R. Edwards, J. A. Hart, K. L. Elmore, and P. Markowski, 2003: Close proximity soundings within supercell environments obtained from the Rapid Update Cycle. *Wea. Forecasting*, **18**, 1243-1261.

Trapp, R. J., E. D. Mitchell, G. A. Tipton, D. W. Effertz, A. I. Watson, D. L. Andra Jr., and M. A. Magsig, 1999: Descending and nondescending tornadic vortex signatures detected by WSR-88Ds. *Wea. Forecasting,* **14,** 625–639.

_____, and M. L. Weisman, 2003: Low-level mesovortices within squall lines and bow echoes. Part II: Their genesis and implications. *Mon. Wea. Rev.*, **131**, 2804–2823.

_____, S. A. Tessendorf, E. S. Godfrey, and H. E. Brooks, 2005: Tornadoes from squall lines and bow echoes. Part I: Climatological distribution. Wea. Forecasting, 20, 23–34.

Wakimoto, R. M., H. V. Murphey, C. A. Davis, and N. T. Atkins, 2006b: High winds generated by bow echoes. Part II: The relationship between the mesovortices and damaging straight-line winds. Mon. Wea. Rev., 134, 2813–2829.

Wheatley, D. M., R. J. Trapp, and N. T. Atkins, 2006: Radar and damage analysis of severe bow echoes during BAMEX. *Mon. Wea. Rev.* , **134**, 791-806.

Weisman, M. L. and R. W. Przybylinski, 1999: Mesoscale convective systems: Squall lines and bow echoes, COMET CBL module, UCAR.

_____, and R. J. Trapp, 2003: Low-level mesovortices within squall lines and bow echoes. Part I: Overview and dependence on environmental shear. *Mon. Wea. Rev.*, **131**, 2779–2803.